Electronic Supplementary Material (ESI) for Chemical Communications.

Supporting Information

A dinuclear copper(II) complex with photoswitchable catechol oxidation activity

Michela Marcon[‡], Stefano Crespi[§], Andreas Pielmeier[‡] and Burkhard König[‡]

[‡]*Faculty of Chemistry and Pharmacy, University of Regensburg, Universitätsstraße 31, 93053 Regensburg, Germany*

[§]*Department of Chemistry, Ångström Laboratories, Uppsala University, Box 523, 751 20 Uppsala, Sweden*

E-mail: burkhard.koenig@ur.de

Table of Contents

A. General Information 3

B. Synthesis of the ligand 4

B.1. 1-methyl-4-nitrosobenzene (2a) 4

B.2. 1-methyl-3-nitrosobenzene (2b) 4

B.3. (*E*)-1,2-di-*p*-tolyldiazene (3a) 4

B.4. (*E*)-1,2-di-*m*-tolyldiazene (3b) 4

B.5. (*E*)-1-phenyl-2-(*p*-tolyl)diazene (3c) 4

B.6. (*E*)-1,2-bis(4-(bromomethyl)phenyl)diazene (4a) 5

B.7. (*E*)-1,2-bis(3-(bromomethyl)phenyl)diazene (4b) 5

B.8. (*E*)-1-(4-(bromomethyl)phenyl)-2-phenyldiazene (4c) 5

B.9. (*E*)-1,1'-(diazene-1,2-diylbis(4,1-phenylene))bis(N,N-bis(pyridin-2-ylmethyl)methanamine) (5a) 5

B.10. (*E*)-1,1'-(diazene-1,2-diylbis(3,1-phenylene))bis(N,N-bis(pyridin-2-ylmethyl)methanamine) (5b) 5

B.11. (*E*)-N-(4-(phenyldiazenyl)benzyl)-1-(pyridin-2-yl)-N-(pyridin-2-ylmethyl)methanamine (5c) 6

B.12. [(*E*)-1,1'-(diazene-1,2-diylbis(4,1-phenylene))bis(N,N-bis(pyridin-2-ylmethyl)methanamine)][$CuCl_2$]$_2$ (1a) 6

B.13. [(*E*)-1,1'-(diazene-1,2-diylbis(3,1-phenylene))bis(N,N-bis(pyridin-2-ylmethyl)methanamine)] [$CuCl_2$]$_2$ (1b) 7

B.14. [(*E*)-N-(4-(phenyldiazenyl)benzyl)-1-(pyridin-2-yl)-N-(pyridin-2-ylmethyl)methanamine] [$CuCl_2$]$_2$ (1c) 7

C. Photophysical properties 8

C.1. UV-vis spectra 8

C.2. Calculation of the PSD 12

D. UV-vis kinetic experiments 14

D.1. Experimental setup 14

D.2. UV-vis kinetics 14

E. Crystallographic data 17

F. NMR spectra 22

G. IR spectra 28

H. Cartesian coordinates 28

I. References 28

A. General Information

Starting materials and reagents were purchased from commercial suppliers (Sigma Aldrich, Alfa Aesar, Acros, Fluka, TCI or VWR) and used without further purification. Solvents were used as p.a. grade or distilled. Dry solvents were dried over molecular sieves. For automated flash column chromatography industrial grade of solvents was used. All NMR spectra were measured at room temperature using a Bruker Avance 300 (300 MHz for ^{1}H, 75 MHz for ^{13}C, 282 MHz for ^{19}F) or a Bruker Avance 400 (400 MHz for ^{1}H, 101 MHz for ^{13}C, 376 MHz for ^{19}F) NMR spectrometer. All chemical shifts are reported in δ-scale as parts per million [ppm] (multiplicity, coupling constant J, number of protons) relative to the solvent residual peaks as the internal standard. Coupling constants J are given in Hertz [Hz]. Abbreviations used for signal multiplicity: ^{1}H-NMR: b = broad, s = singlet, d = doublet, t = triplet, q = quartet, hept = heptet dd = doublet of doublets, dt = doublet of triplets, dq = doublet of quartets, and m = multiplet; ^{13}C-NMR: (+) = primary/tertiary, (–) = secondary, (C_q) = quaternary carbon. HRMS (high resolution mass spectra) and LRMS (low resolution mass spectra) were measured at the Central Analytical Laboratory of the University of Regensburg. These mass spectra were recorded on a Finnigan MAT 95, ThermoQuest Finnigan TSQ 7000, Finnigan MAT SSQ 710 A or an Agilent Q-TOF 6540 UHD instrument. Analytical TLC was performed on silica gel coated alumina plates (MN TLC sheets ALUGRAM® Xtra SIL G/UV254). Visualization was done by UV light (254 or 366 nm). If necessary, ninhidrin was used for chemical staining. Purification by column chromatography was performed with silica gel 60 M (40-63 µm, 230-440 mesh, Merck) or with a pre-packed Biotage® Snap Ultra HP-SphereTM 25 µm column on a Biotage® IsoleraTM Spektra One device. FTIR spectroscopy was carried out on a Cary 630 FTIR Spectrometer and the wave numbers are reported as cm^{-1}. For irradiation with UV light Luminus SST-10 UV LT-4787(UV, λ_{max} = 365 nm, I_{max} = 500 mA, 875mW) was used. For irradiation with blue light ILH-XC01-S410-SC211-WIR200 (blue, λ_{max} = 410 nm, I_{max} = 350 mA, 440mW) was used. UV-Vis absorption spectroscopy was performed at 25°C on a Varian Cary 50 Spectrometer and a Varian Cary 4000 Spetrometer with a 10 mm quartz cuvette. UV-vis absorption kinetics were performed at 25°C on an Agilent 8453 spectrometer with a 10 mm gastight quartz cuvette. For temperature control, a Varian Cary Single cell peltier apparatus was used. The lifetime was measured on a FLUOstar Omega well-plate reader with a Greiner 96 F-bottom well plate covered with an adhesive film to avoid evaporation of the solvent. Computational analysis was employed to optimize the structure of the reduced form of ***Z*-1a**, ***E*-1b**, ***Z*-1b**, ***E*-1c** and ***Z*-1c** interacting with molecular oxygen. The geometries was optimized at the r^{2}SCAN-3c level of theory[1] as implemented in the ORCA 5.0.3 software.[2] The nature of the stationary point was confirmed by means of frequency calculations.

B. Synthesis of the ligand

B.1. 1-methyl-4-nitrosobenzene (2a)

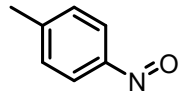

Synthesized according to literature reports.[3] *p*-toluidine (2 g, 18.7 mmol, 1 eq) was dissolved in 40 mL of DCM. To this solution, oxone (11.47 g, 18.7 mmol, 1 eq) dissolved in 50 mL of water was added. The solution immediately turned green and was stirred for 30 min. The crude was extracted with water and DCM. The organic phase was dried over $MgSO_4$ and concentrated, and the green solution was used for the next step without purification.

^{1}H-NMR (300 MHz, Chloroform-*d*): δ 7.81 (d, 2H), 7.39 (d, 2H), 2.45 (s, 3H).

B.2. 1-methyl-3-nitrosobenzene (2b)

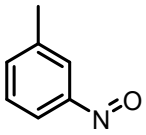

Synthesised following the same procedure as **2a**, starting from *m*-toluidine at 0°C. Green solution used without purification for the next step.

^{1}H NMR (300 MHz, Chloroform-*d*): δ 7.78 (dt, J = 7.1, 2.0 Hz, 1H), 7.64 (s, 1H), 7.56 – 7.49 (m, 2H), 2.50 (s, 3H).

B.3. (*E*)-1,2-di-*p*-tolyldiazene (3a)

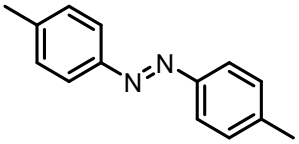

1-methyl-4-nitrosobenzene **2a** (800 mg, 6.60 mmol, 1 eq) and p-toluidine (1 eq) were dissolved in 10 mL of acetic acid. The solution was stirred at room temperature overnight. The mixture was extracted with saturated $NaHCO_3$ and ethyl acetate, washed once with brine and dried. The product was then purified by flash column chromatography (100% PE). The eluate was concentrated by rotary evaporation and an orange solid was obtained in 74% yield.

^{1}H-NMR (300 MHz, Chloroform-*d*): δ 7.81 (d, 2H), 7.30 (d, 2H), 2.43 (s, 3H).

B.4. (*E*)-1,2-di-*m*-tolyldiazene (3b)

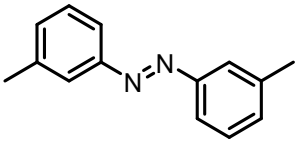

Synthesized following the same procedure as **3a**, starting from **2b**. Orange solid 20% yield.

^{1}H NMR (400 MHz, Chloroform-*d*): δ 7.76 – 7.69 (m, 4H), 7.45 – 7.38 (m, 2H), 7.29 (d, J = 7.5 Hz, 2H), 2.46 (s, 6H).

B.5. (*E*)-1-phenyl-2-(*p*-tolyl)diazene (3c)

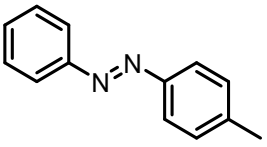

Synthesized following the same procedure as **3a**, starting from commercial nitrosobenzene and *p*-toluidine. Orange solid, 92% yield.

^{1}H NMR (400 MHz, Chloroform-*d*): δ 7.91 (d, J = 7.1 Hz, 2H), 7.84 (d, J = 8.3 Hz, 2H), 7.56 – 7.42 (m, 3H), 7.32 (d, J = 8.0 Hz, 2H), 2.44 (s, 3H).

B.6. (*E*)-1,2-bis(4-(bromomethyl)phenyl)diazene (4a)

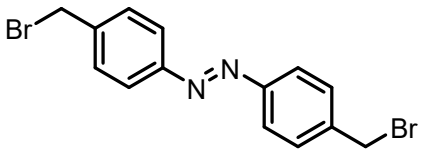

Synthesized according to literature report.[4] To a solution of (*E*)-1,2-di-p-tolyldiazene **3a** (420 mg, 2 mmol, 1 eq) in 20 mL

of dry acetonitrile was added N-bromosuccinimide (2.3 eq) and AIBN (0.08 eq). The solution was stirred overnight at 70°C. The volume was reduced by rotary evaporation. The precipitate was filtered and washed with abundant MeOH. Orange solid, 77% yield.

^{1}H-NMR (300 MHz, Chloroform-*d*): δ 7.87 (d, 2H), 7.55 (d, 2H), 4.56 (s, 4H).

B.7. (*E*)-1,2-bis(3-(bromomethyl)phenyl)diazene (4b)

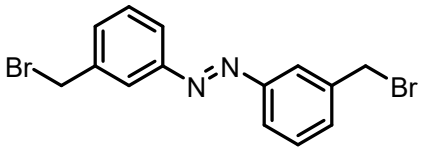

Synthesized following the same procedure as **4a**, starting from **3b**. Orange solid, yield 50%.

^{1}H NMR (300 MHz, Chloroform-*d*): δ 7.95 (d, J = 1.6 Hz, 2H), 7.92 – 7.81 (m, 2H), 7.52 (dd, J = 4.8, 1.5 Hz, 4H), 4.59 (s, 4H).

B.8. (*E*)-1-(4-(bromomethyl)phenyl)-2-phenyldiazene (4c)

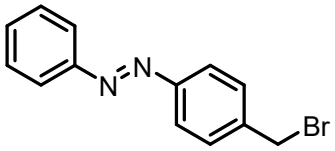

Synthesized following the same procedure as **4a**, starting from **3c**. Orange solid, yield 50%.

^{1}H NMR (400 MHz, Chloroform-*d*): δ 7.95 – 7.85 (m, 4H), 7.58 – 7.45 (m, 5H), 4.56 (s, 2H).

B.9. (*E*)-1,1'-(diazene-1,2-diylbis(4,1-phenylene))bis(N,N-bis(pyridin-2-ylmethyl)methanamine) (5a)

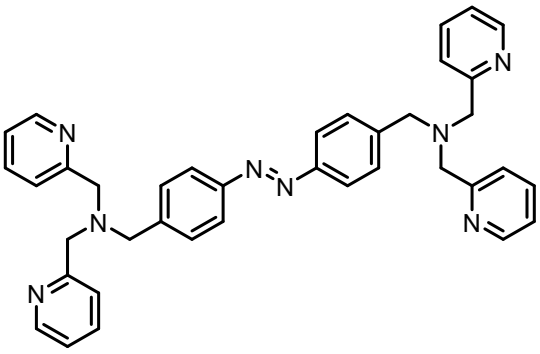

200 mg (1 mmol, 2 eq) of bis(pyridin-2-ylmethyl)amine were dissolved in a crimp capped vial in 8 ml dry DMF. Subsequently, 1 eq of (*E*)-1,2-bis(4-(bromomethyl)phenyl)diazene **4a**, 2 eq of sodium iodide and 2 eq of DIPEA were added. The reaction was stirred over weekend at room temperature. DMF was removed with rotary evaporator and the resulting orange oil was purified by column chromatography (DCM:MeOH 9:1) to obtain an orange solid in 51% yield.

^{1}H-NMR (400 MHz, Methanol-*d*4): δ 8.43 (dd, 4H), 7.83-7.79 (m, 8H), 7.69 (d, 4H), 7.58 (d, 4H), 7.29-7.26 (ddd, 4H), 3.81 (s, 8H), 3.76 (s, 4H).

^{13}C-NMR (101 MHz, Methanol-*d*4): δ 159.0, 151.9, 148.0, 142.1,137.4, 129.4, 123.5, 122.5, 122.4, 59.5, 58.1.

HRMS (ESI-MS): m/z calc. for $[C_{38}H_{38}N_8]^{2+}$ $[M2H]^{2+}$ 303.1604, found 303.1612.

B.10. (*E*)-1,1'-(diazene-1,2-diylbis(3,1-phenylene))bis(N,N-bis(pyridin-2-ylmethyl)methanamine) (5b)

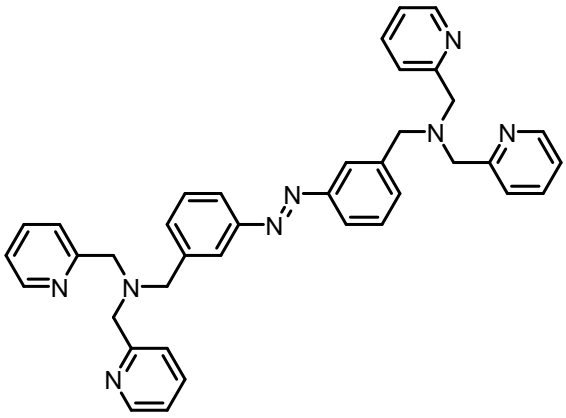

Synthesized following the same procedure as **5a**, starting from **4b**. Sticky orange oil, yield 80%.

^{1}H NMR (400 MHz, Methanol-*d*4): δ 8.45 (ddd, J = 5.0, 1.6, 0.8 Hz, 4H), 7.95 (s, 2H), 7.86 – 7.78 (m,

6H), 7.72 (d, J = 7.9 Hz, 4H), 7.59 (d, J = 7.6 Hz, 2H), 7.51 (t, J = 7.7 Hz, 2H), 7.28 (ddd, J = 7.4, 5.0, 1.1 Hz, 4H), 3.86 (s, 8H), 3.82 (s, 4H).

^{13}C NMR (101 MHz, Methanol-*d*4): δ 159.0, 152.7, 148.1, 140.0, 137.4, 131.5, 128.9, 123.45, 122.8, 122.5, 121.5, 59.5, 58.2.

HRMS (ESI-TOF) m/z calculated for $[C_{38}H_{38}N_8]^{2+}$ $[M2H]^{2+}$ 303.1604, found 303.1613

B.11. (*E*)-N-(4-(phenyldiazenyl)benzyl)-1-(pyridin-2-yl)-N-(pyridin-2-ylmethyl)methanamine (5c)

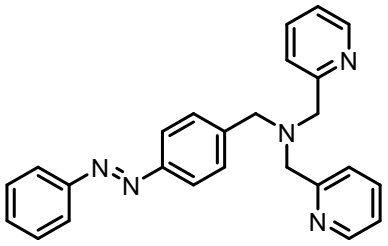

Synthesized following the same procedure as **5a**, starting from **4c**. Sticky orange solid, yield 55%.

^{1}H NMR (400 MHz, Methanol-*d*4): δ 8.44 (d, J = 5.0 Hz, 2H), 7.85 (dt, J = 22.5, 8.1 Hz, 6H), 7.70 (d, J = 7.8 Hz, 2H), 7.59 (d, J = 8.2 Hz, 2H), 7.56 – 7.46 (m, 3H), 7.33 – 7.24 (m, 2H), 3.82 (s, 4H), 3.76 (s, 2H).

^{13}C NMR (101 MHz, Methanol-*d*4): δ 154.0, 153.2, 149.5, 143.6, 138.8, 132.2, 130.8, 130.3, 124.9, 123.9, 123.9, 123.8, 60.9, 59.5.

HRMS (ESI-TOF) m/z calculated for $[C_{25}H_{24}N_5]^{+}$ $[MH]^{+}$ 394.2026, found 394.2031

B.12. [(*E*)-1,1'-(diazene-1,2-diylbis(4,1-phenylene))bis(N,N-bis(pyridin-2-ylmethyl)methanamine)][$CuCl_2$]$_2$ (1a)

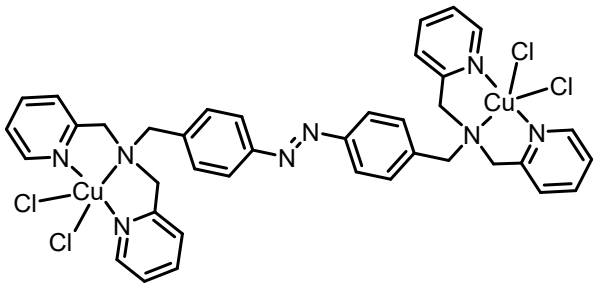

(*E*)-1,1'-(diazene-1,2-diylbis(4,1-phenylene))bis(*N*,*N*-bis(pyridin-2-ylmethyl)methanamine) **5a** was dissolved in the minimum amount of MeOH and $CuCl_2$ dissolved in minimum amount of MeOH was added while stirring. The mixture immediately turned dark green and was left stirring for 24 hours at room temperature, then filtered. A green solid was obtained, which was recrystallized with MeOH:diethyl ether. 92% yield.

B.13. [(*E*)-1,1'-(diazene-1,2-diylbis(3,1-phenylene))bis(N,N-bis(pyridin-2-ylmethyl)methanamine)] [$CuCl_2$]$_2$ (1b)

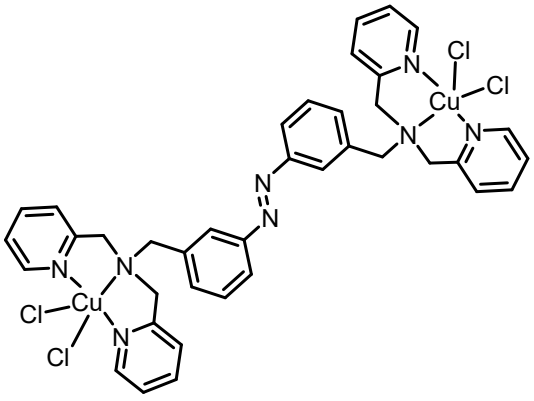

Synthesized following the same procedure as **1a**, starting from **5b**. Recrystallized with MeOH:diethyl ether. Green solid, 98% yield.

B.14. [(*E*)-N-(4-(phenyldiazenyl)benzyl)-1-(pyridin-2-yl)-N-(pyridin-2-ylmethyl)methanamine] [$CuCl_2$] (1c)

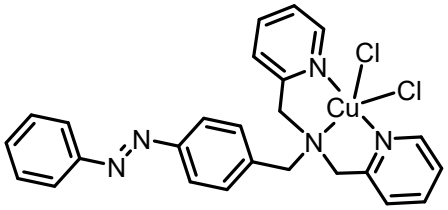

Synthesized following the same procedure as **1a**, starting from **5c**. Recrystallized with MeOH:diethyl ether. Dark green solid, 82% yield.

C. Photophysical properties

C.1. UV-vis spectra

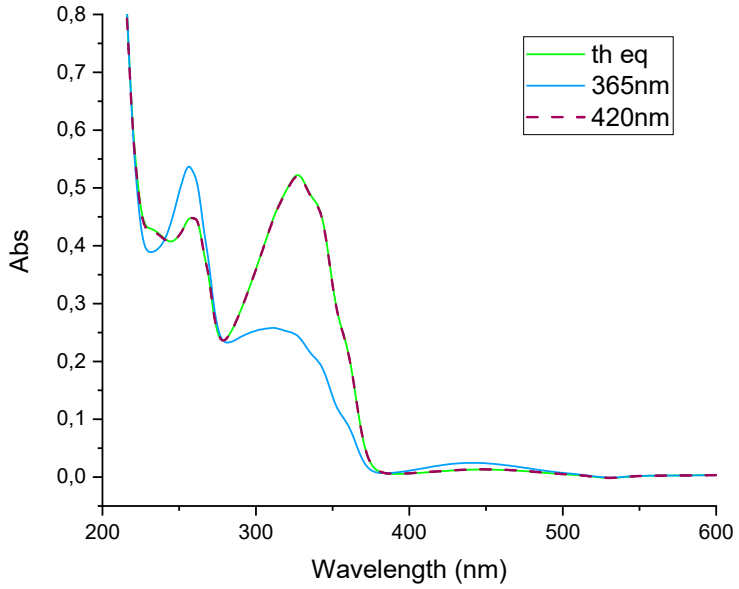

Figure S- 1. Absorption spectra of **1a** 25 µM in MeOH.

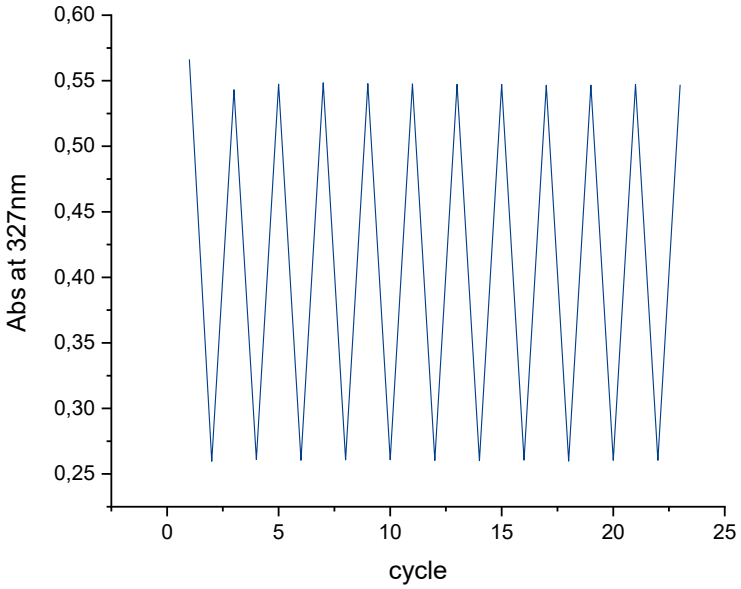

Figure S- 2. Fatigue resistance of **1a** 25 µM in MeOH.

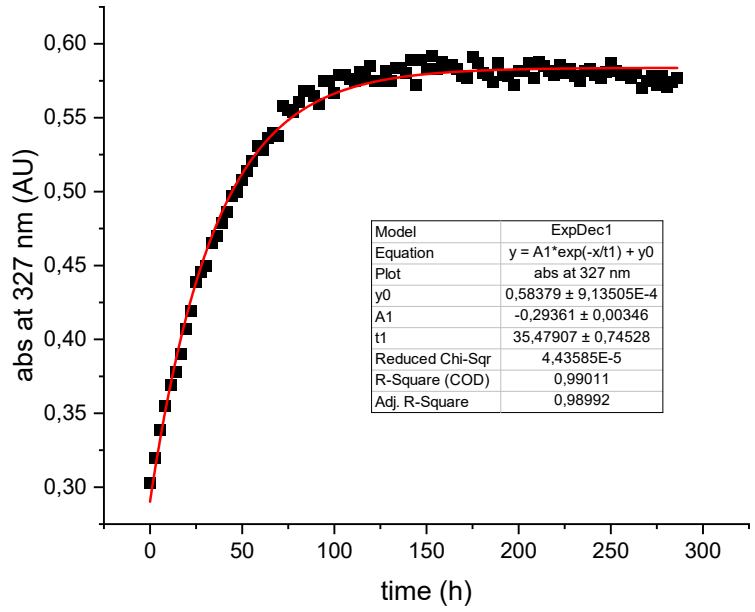

Figure S- 3. Thermal half life measurement of **1a** 25 µM in MeOH after irradiation with 365 nm LED.

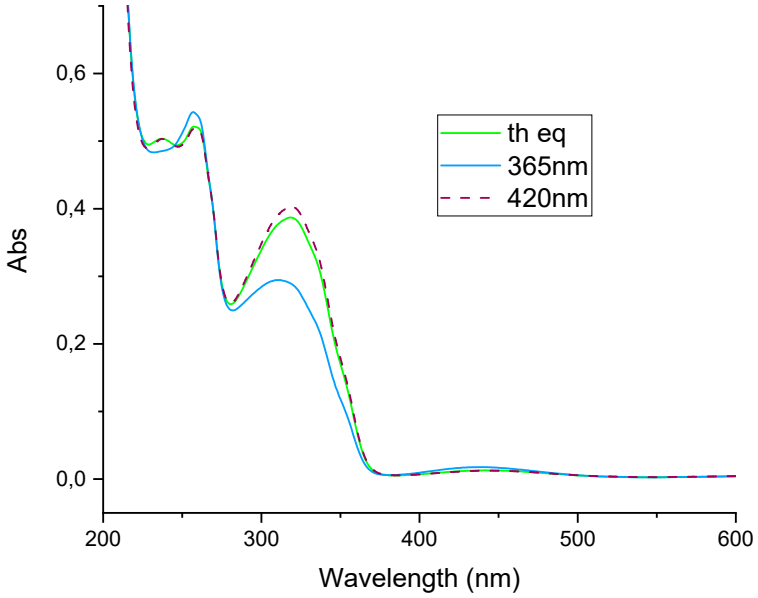

Figure S- 4. Absorption spectra of **1b** 25 µM in MeOH.

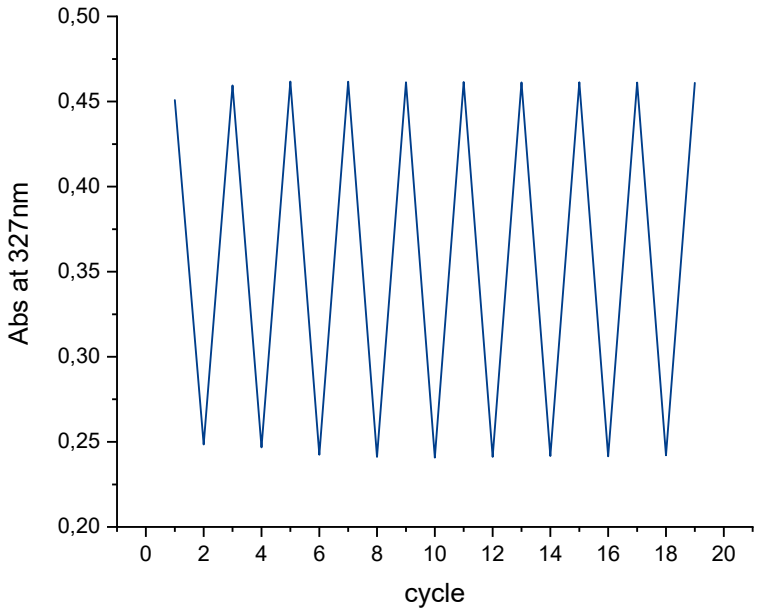

Figure S- 5. Fatigue resistance of **1b** 25 µM in MeOH.

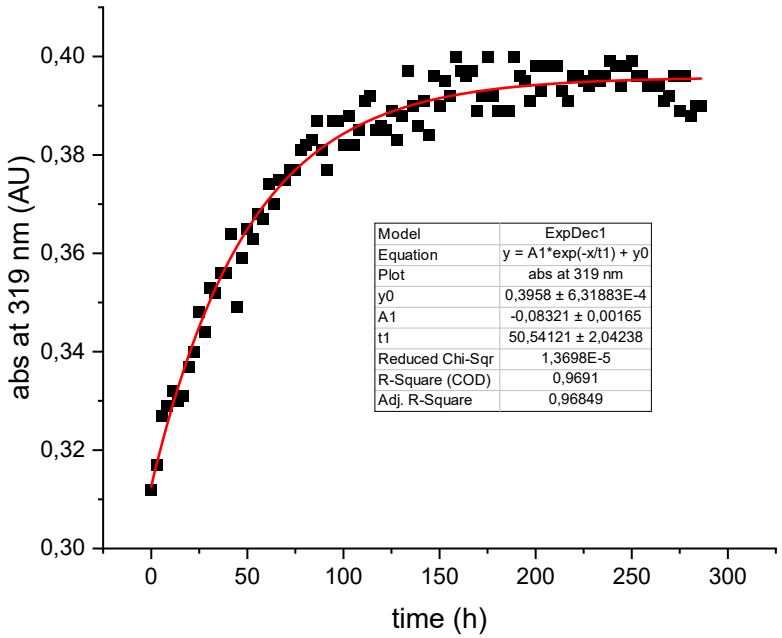

Figure S- 6. Thermal half life measurement of **1b** 25 µM in MeOH after irradiation with 365 nm LED.

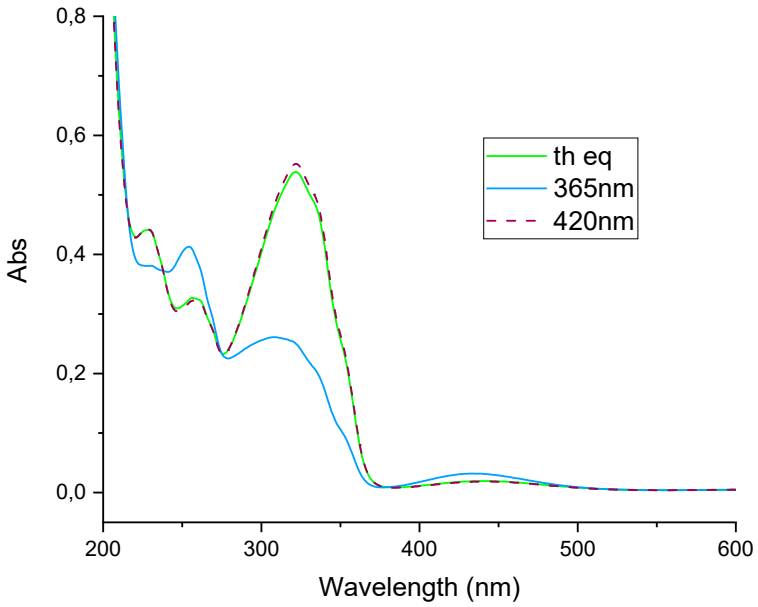

Figure S- 7. Absorption spectra of **1c** 25 µM in MeOH.

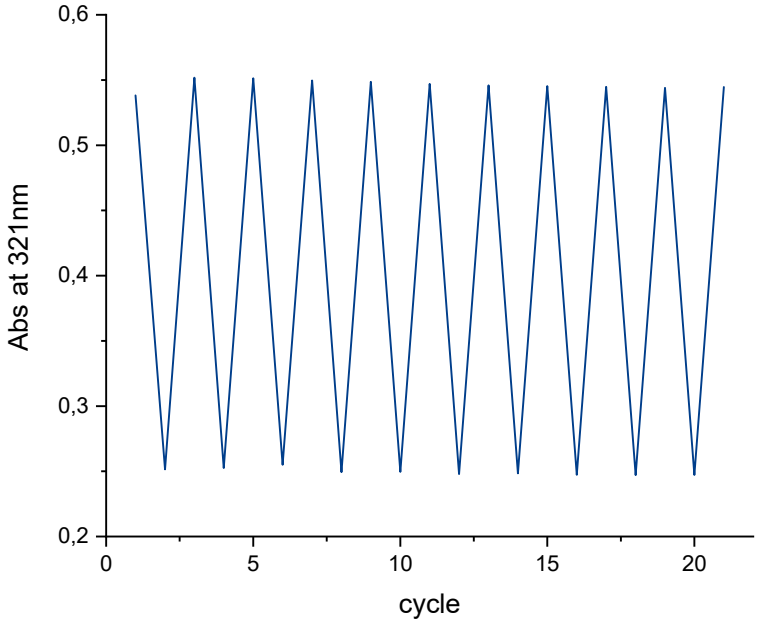

Figure S- 8. Fatigue resistance of **1c** 25 µM in MeOH.

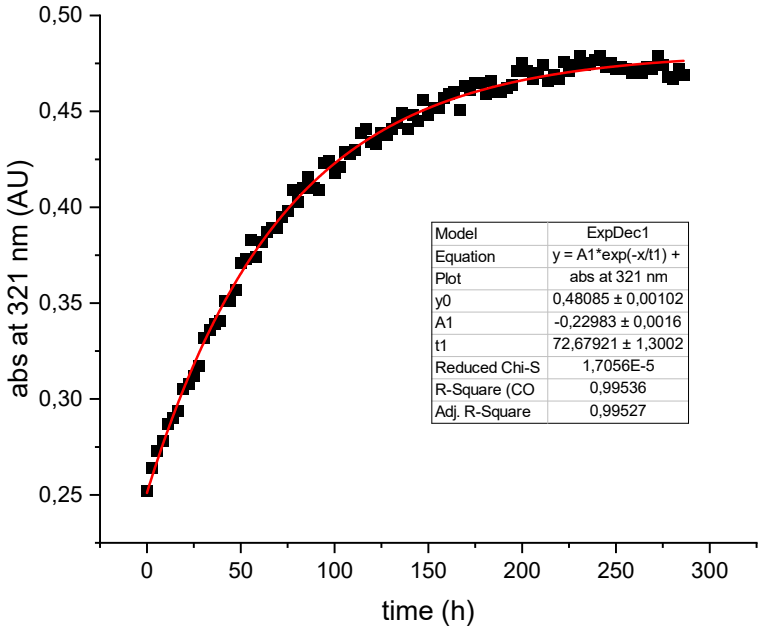

Figure S- 9. Thermal half life measurement of **1c** 25 µM in MeOH after irradiation with 365 nm LED.

C.2. Calculation of the PSD

For the calculation of the photostationary distribution (PSD) a reported method is used.[5] For **1a**: the spectrum at the thermal equilibrium is approximated to 100% of the *E*-isomer. The spectrum at the thermal equilibrium is fitted with four gaussian functions using the program OriginLab. The center of peak 3 is fixed for the fitting of the function at 365 nm. The ratio between the two areas gives an approximate PSD which is used to calculate the spectrum of pure *Z*. The spectra of the thermal equilibrium and 100% *Z* are then combined until they fit the experimental spectrum for 365 nm, giving the distribution of the two isomers. Similar procedures are used for **1b** and **1c**.

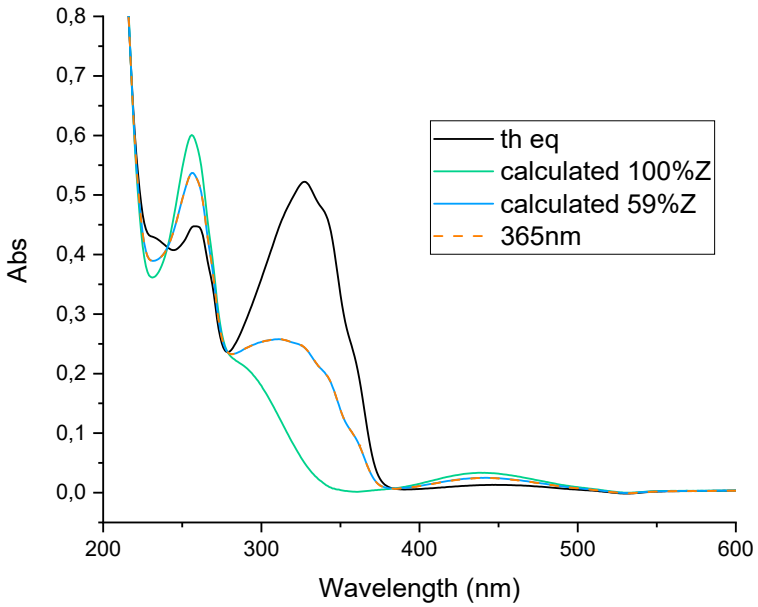

Figure S- 10. Simulated spectra and calculated PSD for **1a**.

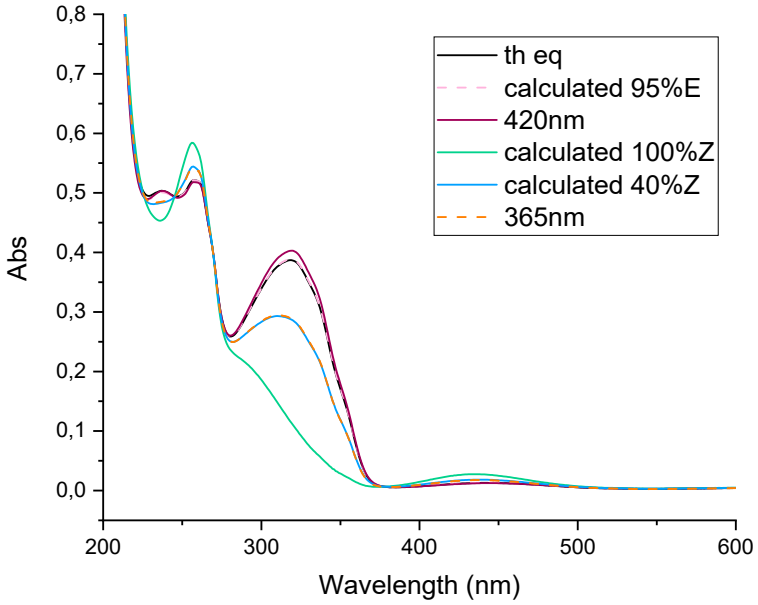

Figure S- 11. Simulated spectra and calculated PSD for **1b**.

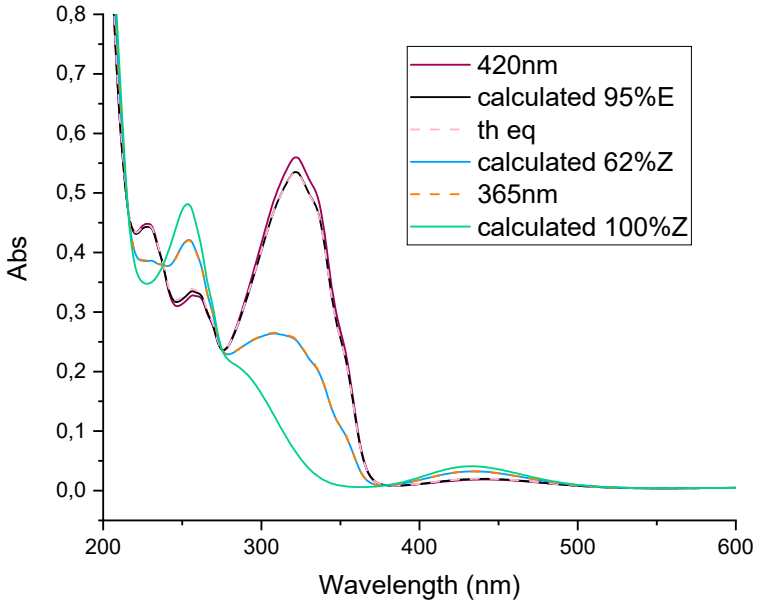

Figure S- 12. Simulated spectra and calculated PSD for **1c**.

Table S- 1. Photophysical properties of the photoswitchable complexes.

	λ_{max} ππ* *E-isomer*	ε [$M^{-1}cm^{-1}$] *E-isomer*	λ_{max} nπ* *Z-isomer*	ε [$M^{-1}cm^{-1}$] *Z-isomer*	*PSD th. eq. (E:Z)*	*PSD 365 nm (E:Z)*	*PSD 420 nm (E:Z)*	*t½ (h) Z→E*
1a	327 nm	21100 ± 600	440 nm	990 ± 30	100:0	41:59	100:0	24.5
1b	319 nm	16600 ± 500	440 nm	750 ± 30	95:5	60:40	100:0	35.0
1c	321 nm	21100 ± 500	435 nm	1200 ± 30	95:5	39:61	100:0	50.3

D. UV-vis kinetic experiments

D.1. Experimental setup

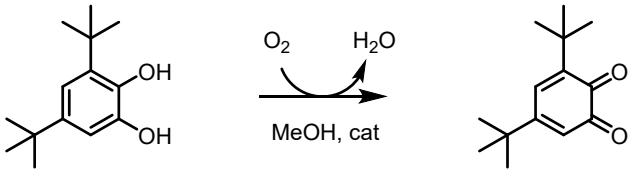

2 mL of catalyst solution (**1a** or **1b**) 10 µM in MeOH saturated with O_2 is added in a gastight cuvette equipped with a stirring bar. For the experiments with the *Z*-isomer the cuvette is irradiated with a 365 nm LED for 30 seconds, while for the experiments with the *E*-isomer the cuvette is left in the dark. 20 µL of a freshly made solution of di-*tert*-butylcatechol 1M in MeOH is added to the cuvette (to give a final concentration of 0.02M) and measurement is started immediately. In case of $CuCl_2$, ***E*-1c** and ***Z*-1c** a double concentration is used. The formation of di-*tert*-butyl-quinone (DTBQ) is followed at 400 nm and the absorption of the catalysts at 400 nm is subtracted. The kinetic traces for all compounds are shown in ***Figure S- 13***.

For the Michaelis-Menten study, the same procedure is used with increasing concentration of di-*tert*-butyl-cathechol is used. The rate is calculated with the initial rates method and plotted against the initial concentration of di-*tert*-butyl-catechol. The plots for the *E*- and *Z*-configurations are shown in ***Figure S- 15*** and ***Figure S- 16*** and the values of K_M, v_{max}, k_{cat}, TON (300 s) and k_{obs} are reported in ***Table S- 2***. k_{cat} is calculated according to the equation

$$k_{cat} = \frac{v_{max}}{[E]}$$

Where v_{max} is extrapolated from the Michaelis Menten plot and [E] is the enzyme concentration. k_{obs} is extrapolated from the pseudo-first order approximation of the kinetic traces (shown in ***Figure S- 14***).

D.2. UV-vis kinetics

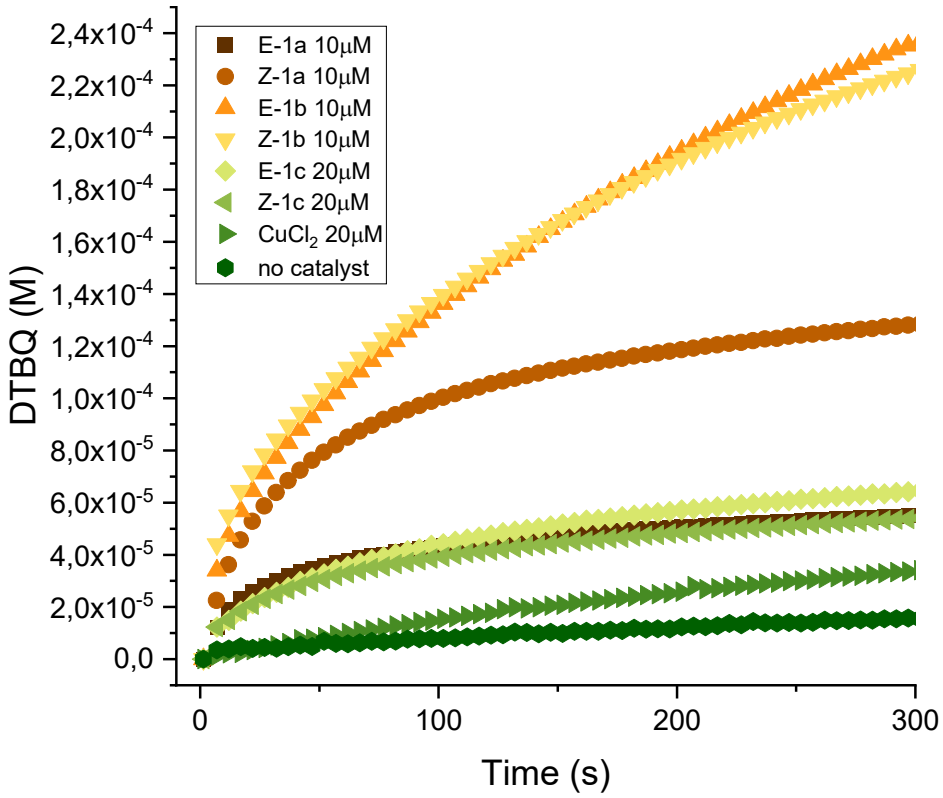

Figure S- 13: Comparison of the reaction kinetics of all the species studied.

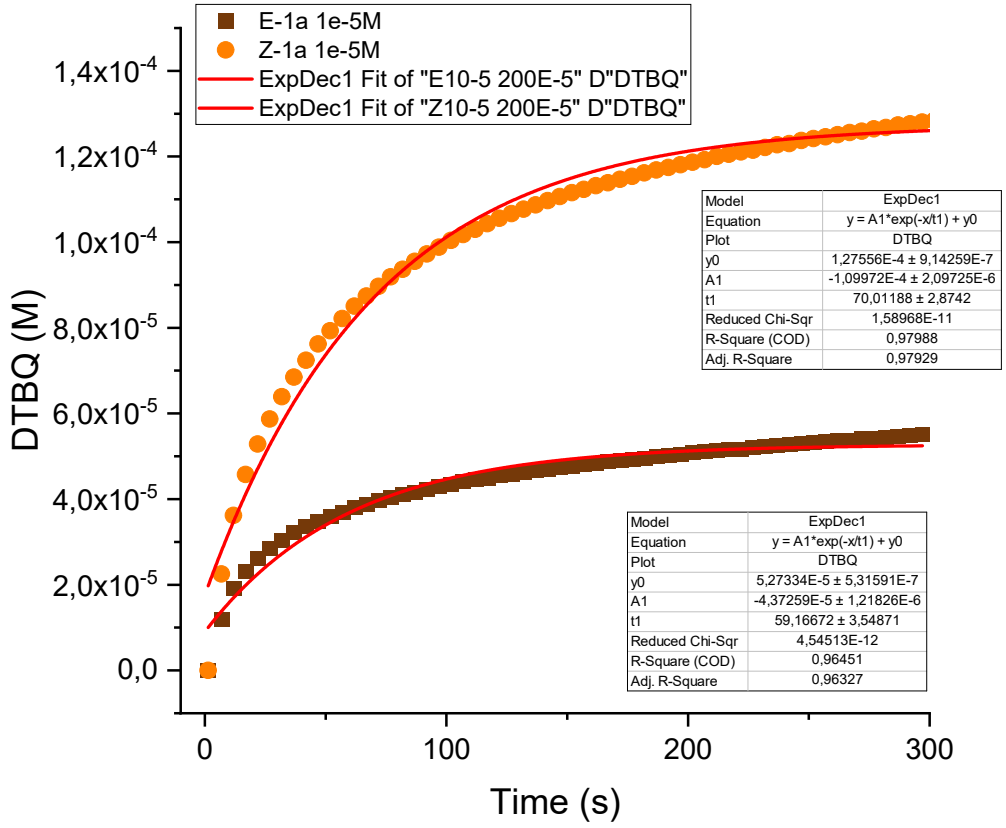

Figure S- 14: Highlighted kinetic traces of catalysts ***E*-1a** and ***Z*-1a** with *pseudo*-first order approximation.

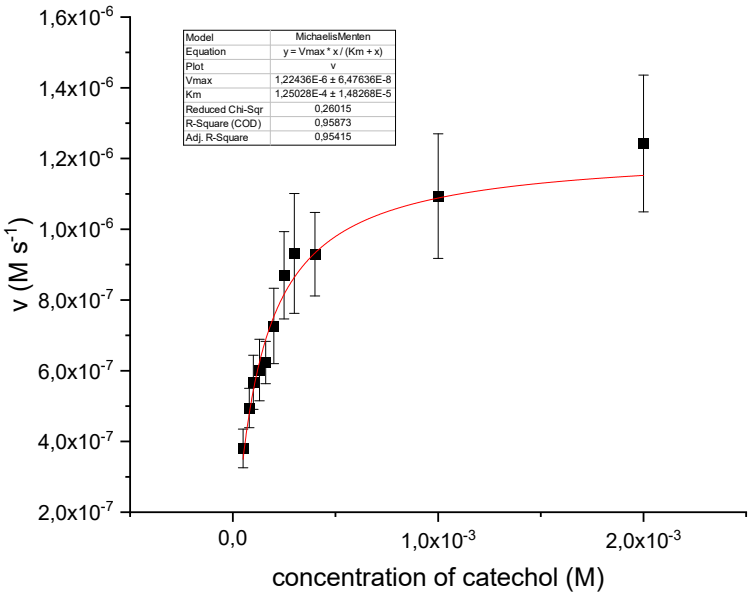

Figure S- 15: Michaelis-Menten plot for ***E*-1a**.

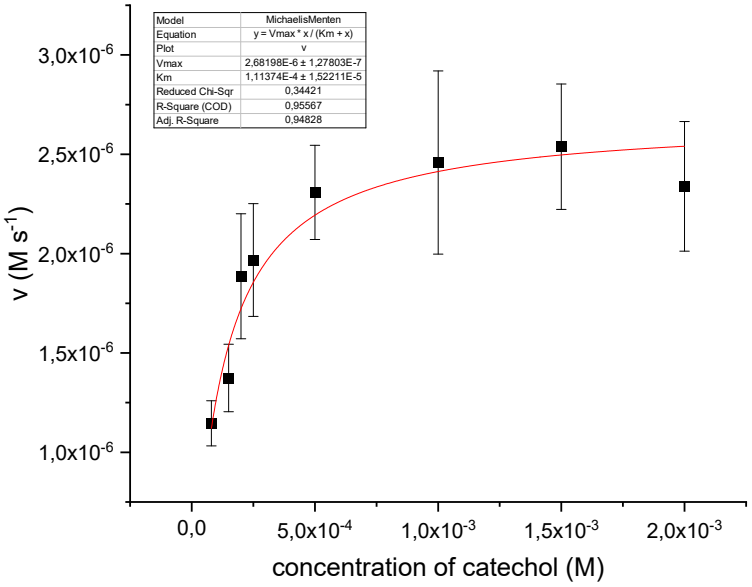

Figure S- 16: Michaelis-Menten plot for ***Z*-1a**.

Table S- 2. Kinetic constants for the switchable catalist **1a**.

catalyst	K_M (M)	v_{max} (Ms^{-1})	k_{cat} (s^{-1})	k_{obs} (s^{-1})	TON at 300 s
***E*-1a**	$1.25*10^{-4} \pm 0.15*10^{-4}$	$1.22*10^{-6} \pm 0.06*10^{-6}$	$1.22*10^{-1} \pm 0.06*10^{-1}$	$1.69*10^{-4} \pm 0.10*10^{-4}$	5.5
***Z*-1a**	$1.11*10^{-4} \pm 0.15*10^{-4}$	$2.68*10^{-6} \pm 0.13*10^{-6}$	$2.68*10^{-1} \pm 0.13*10^{-1}$	$1.43*10^{-4} \pm 0.04*10^{-4}$	12.8

E. Crystallographic data

Experimental. Single clear green prism-shaped crystals of ***E*-1a** were used as supplied. A suitable crystal with dimensions 0.23 × 0.21 × 0.12 mm^3 was selected and mounted on a MITIGEN holder with inert oil on a XtaLAB Synergy R, DW system, HyPix-Arc 150 diffractometer. The crystal was kept at a steady T = 123.01(10) K during data collection. The structure was solved with the **ShelXT** 2018/2[6] solution program using dual methods and by using **Olex2** 1.3-alpha[7] as the graphical interface. The model was refined with **ShelXL** 2018/3[8] using full matrix least squares minimization on F^2.

Crystal Data. $C_{38}H_{36}Cl_4Cu_2N_8$, M_r = 873.63, monoclinic, $P2_1/c$ (No. 14), a = 9.44092(4) Å, b = 11.74337(5) Å, c = 22.12241(10) Å, β = 100.1219(4)°, $\alpha = \gamma = 90°$, V = 2414.498(18) $Å^3$, T = 123.01(10) K, Z = 2, Z' = 0.5, μ(Cu K_α) = 3.373, 76090 reflections measured, 4956 unique (R_{int} = 0.0254) which were used in all calculations. The final wR_2 was 0.1033 (all data) and R_1 was 0.0347 (I≥2 σ(I)).

Table S- 3. Crystal data and structure refinement for ***E*-1a**.

Compound	***E*-1a**
Formula	$C_{38}H_{36}Cl_4Cu_2N_8$
$D_{calc.}$/ g cm^{-3}	1.202
μ/mm^{-1}	3.373
Formula Weight	873.63
Colour	clear green
Shape	prism-shaped
Size/mm^3	0.23×0.21×0.12
T/K	123.01(10)
Crystal System	monoclinic
Space Group	$P2_1/c$
a/Å	9.44092(4)
b/Å	11.74337(5)
c/Å	22.12241(10)
α/°	90
β/°	100.1219(4)
γ/°	90
V/$Å^3$	2414.498(18)
Z	2
Z'	0.5
Wavelength/Å	1.54184
Radiation type	Cu K_α
Θ_{min}/°	4.060
Θ_{max}/°	74.994
Measured Refl's.	76090
Indep't Refl's	4956
Refl's I≥2 σ(I)	4851
R_{int}	0.0254
Parameters	275
Restraints	0
Largest Peak	0.955
Deepest Hole	-0.395
GooF	1.156
wR_2 (all data)	0.1033
wR_2	0.1030
R_1 (all data)	0.0351
R_1	0.0347

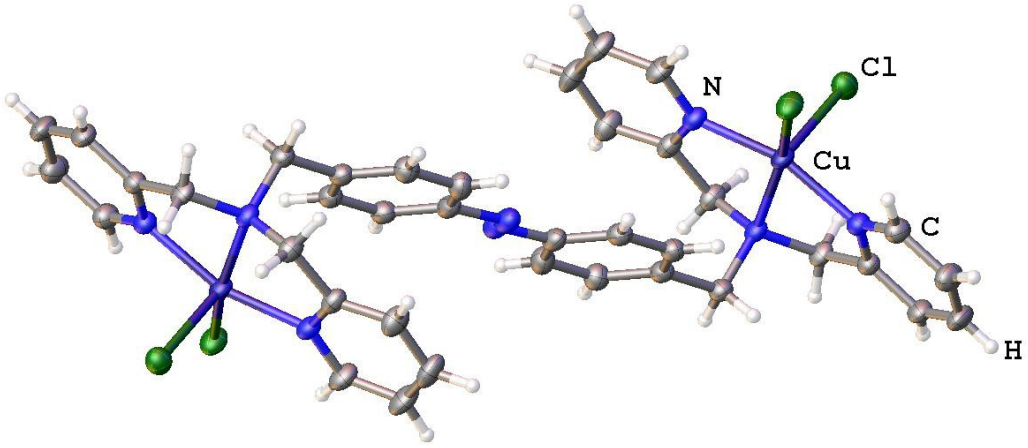

Figure S- 17. Crystal structure of ***E*-1a**.

Figure S- 18. Images of the crystal on the diffractometer.

Table S- 4. Fractional Atomic Coordinates (×10^4) and Equivalent Isotropic Displacement Parameters (Å^2×10^3) for ***E*-1a**. U_{eq} is defined as 1/3 of the trace of the orthogonalised U_{ij}.

Atom	x	y	z	U_{eq}
Cu01	5692.8(3)	4117.2(2)	6972.8(2)	24.81(10)
Cl02	5148.6(5)	4451.1(4)	8043.2(2)	32.60(12)
Cl03	7152.1(5)	2583.1(4)	7034.4(2)	34.43(13)
N004	4479.1(15)	5469.0(13)	6578.1(7)	23.7(3)
N005	3824.6(16)	3301.5(13)	6649.4(7)	26.0(3)
N006	7237.1(15)	5306.8(14)	7110.7(7)	26.9(3)
C008	6749.4(19)	6373.6(17)	7028.2(8)	28.0(4)
C009	5138(2)	6509.0(16)	6886.0(9)	28.2(4)
C00A	5823.6(19)	5527.3(17)	5692.4(8)	27.1(4)
C00B	2677.2(19)	4006.3(16)	6567.4(8)	26.3(4)
C00C	4385.0(19)	5554.3(16)	5895.5(8)	27.2(4)
C00D	3015.3(18)	5238.3(16)	6709.4(9)	26.6(4)
C00E	7821(2)	4428.7(17)	5453.2(8)	29.2(4)
C00F	8456.8(19)	5434.8(18)	5295.4(8)	30.6(4)
C00G	1294(2)	3601.4(19)	6363.7(9)	31.8(4)
C00H	6516(2)	4483.2(17)	5650.1(8)	28.7(4)
C00I	3634(2)	2194.3(17)	6522.0(9)	31.8(4)
C00J	7791(2)	6480.3(19)	5339.4(9)	33.9(4)
C00K	8667(2)	5127.1(19)	7264.9(10)	33.9(4)
C00L	7675(2)	7301.6(19)	7085.6(10)	35.5(4)
C00M	1096(2)	2460(2)	6233.2(11)	39.8(5)
C00N	6467(2)	6521.8(18)	5533.3(9)	32.0(4)
C00O	9141(2)	7109(2)	7243.9(11)	40.9(5)
C00P	2279(2)	1741.4(19)	6310.0(11)	39.5(5)
C00Q	9640(2)	6009(2)	7340.7(11)	39.5(5)
N1	9791.5(17)	5474.2(16)	5073.8(7)	33.8(4)

Table S- 5. Anisotropic Displacement Parameters (×10^4) for ***E*-1a**. The anisotropic displacement factor exponent takes the form: $-2\pi^2[h^2a^{*2} \times U_{11} + ... + 2hka^* \times b^* \times U_{12}]$.

Atom	U_{11}	U_{22}	U_{33}	U_{23}	U_{13}	U_{12}
Cu01	15.47(15)	28.41(17)	29.69(16)	1.13(10)	1.6(1)	0.83(9)
Cl02	35.1(2)	31.3(2)	31.8(2)	-0.50(17)	6.72(18)	-2.09(17)
Cl03	21.8(2)	31.4(2)	49.1(3)	4.56(19)	3.51(18)	5.21(16)
N004	15.2(7)	28.2(7)	27.8(7)	-1.2(6)	3.5(5)	0.1(5)
N005	19.4(7)	31.1(8)	27.1(7)	2.5(6)	2.8(5)	0.3(6)
N006	17.6(7)	34.0(8)	28.5(7)	-2.1(6)	2.4(6)	-0.7(6)
C008	20.3(8)	34.3(10)	29.4(9)	-5.7(7)	4.1(7)	-3.6(7)
C009	22.4(9)	26.2(9)	35.6(9)	-5.0(7)	3.9(7)	-0.6(7)
C00A	21.4(8)	36.3(10)	23.2(8)	1.1(7)	2.5(6)	-0.6(7)
C00B	20.2(8)	32.6(10)	25.9(8)	3.8(7)	3.0(7)	-0.9(7)
C00C	20.8(8)	33.0(9)	26.9(9)	2.5(7)	2.1(7)	0.3(7)
C00D	15.0(7)	32.1(9)	33.1(9)	-1.2(7)	5.8(6)	1.6(7)
C00E	24.1(9)	37.6(10)	25.3(8)	2.1(7)	2.6(7)	1.6(7)
C00F	21.0(8)	46.4(11)	24.3(8)	0.8(8)	3.3(7)	-3.9(8)
C00G	18.8(8)	41.0(11)	34.0(9)	6.6(8)	0.6(7)	-0.8(8)
C00H	24.5(9)	36.1(10)	25.0(8)	2.2(7)	3.0(7)	-2.0(7)
C00I	28.8(10)	31.0(10)	34.3(9)	3.1(8)	1.7(7)	-0.9(8)
C00J	30.4(10)	39.3(11)	32.9(9)	0.1(8)	8.3(8)	-6.7(8)
C00K	18.5(8)	40.6(11)	41.8(11)	-4.1(9)	2.9(7)	1.1(8)
C00L	29.0(10)	31.2(11)	46.5(11)	-8.8(9)	6.6(8)	-3.1(8)
C00M	25.0(10)	44.4(12)	45.7(12)	7.4(9)	-6.2(8)	-10.8(8)
C00N	29.7(9)	34.4(10)	32.4(9)	1.0(8)	6.6(7)	-0.9(8)
C00O	26.1(10)	44.4(12)	52.6(12)	-15.2(10)	8.4(9)	-12.4(9)
C00P	36.4(11)	31.8(11)	46.8(12)	3.4(9)	-2.0(9)	-7.1(9)
C00Q	18.1(9)	49.7(12)	50.0(12)	-11.4(10)	4.5(8)	-3.2(8)
N1	23.0(8)	50.4(10)	28.3(8)	0.1(7)	5.7(6)	-3.9(7)

Table S- 6. Bond Lengths in Å for E-1a.

Atom	Atom	Length/Å
Cu01	Cl02	2.5402(5)
Cu01	Cl03	2.2575(5)
Cu01	N004	2.0601(15)
Cu01	N005	2.0241(15)
Cu01	N006	2.0035(16)
N004	C009	1.481(2)
N004	C00C	1.501(2)
N004	C00D	1.486(2)
N005	C00B	1.350(2)
N005	C00I	1.336(3)
N006	C008	1.336(3)
N006	C00K	1.349(2)
C008	C009	1.507(2)
C008	C00L	1.389(3)
C00A	C00C	1.504(2)
C00A	C00H	1.400(3)
C00A	C00N	1.390(3)
C00B	C00D	1.503(3)
C00B	C00G	1.389(3)
C00E	C00F	1.397(3)
C00E	C00H	1.379(3)
C00F	C00J	1.391(3)
C00F	N1	1.431(2)
C00G	C00M	1.377(3)
C00I	C00P	1.388(3)
C00J	C00N	1.392(3)
C00K	C00Q	1.374(3)
C00L	C00O	1.385(3)
C00M	C00P	1.386(3)
C00O	C00Q	1.379(3)
N1	N1[1]	1.244(4)

[1]2-x,1-y,1-z

Table S- 7. Bond Angles in ° for ***E*-1a**.

Atom	Atom	Atom	Angle/°
Cl03	Cu01	Cl02	106.752(19)
N004	Cu01	Cl02	95.03(4)
N004	Cu01	Cl03	158.22(4)
N005	Cu01	Cl02	95.52(4)
N005	Cu01	Cl03	97.37(5)
N005	Cu01	N004	80.19(6)
N006	Cu01	Cl02	90.66(5)
N006	Cu01	Cl03	97.31(5)
N006	Cu01	N004	82.12(6)
N006	Cu01	N005	161.70(6)
C009	N004	Cu01	106.44(11)
C009	N004	C00C	110.71(14)
C009	N004	C00D	112.99(14)
C00C	N004	Cu01	114.09(11)
C00D	N004	Cu01	104.11(11)
C00D	N004	C00C	108.43(13)
C00B	N005	Cu01	112.71(12)
C00I	N005	Cu01	127.73(13)
C00I	N005	C00B	119.55(16)
C008	N006	Cu01	114.14(12)
C008	N006	C00K	119.11(17)
C00K	N006	Cu01	126.75(14)
N006	C008	C009	116.01(16)
N006	C008	C00L	121.80(18)
C00L	C008	C009	122.17(18)
N004	C009	C008	109.64(15)
C00H	C00A	C00C	119.66(17)
C00N	C00A	C00C	121.03(17)
C00N	C00A	C00H	119.29(17)
N005	C00B	C00D	115.23(15)
N005	C00B	C00G	121.36(18)
C00G	C00B	C00D	123.41(17)
N004	C00C	C00A	113.73(14)
N004	C00D	C00B	107.78(14)
C00H	C00E	C00F	119.12(18)
C00E	C00F	N1	123.77(19)
C00J	C00F	C00E	120.66(17)
C00J	C00F	N1	115.57(18)
C00M	C00G	C00B	119.11(19)
C00E	C00H	C00A	121.01(18)
N005	C00I	C00P	121.74(19)
C00F	C00J	C00N	119.61(19)
N006	C00K	C00Q	122.0(2)
C00O	C00L	C008	118.7(2)
C00G	C00M	C00P	119.34(19)
C00A	C00N	C00J	120.30(19)
C00Q	C00O	C00L	119.4(2)
C00M	C00P	C00I	118.9(2)
C00K	C00Q	C00O	118.97(19)
N1[1]	N1	C00F	113.5(2)

[1]2-x,1-y,1-z

Table S- 8. Torsion Angles in ° for ***E*-1a**.

Atom	Atom	Atom	Atom	Angle/°
Cu01	N004	C009	C008	35.98(17)
Cu01	N004	C00C	C00A	-51.69(18)
Cu01	N004	C00D	C00B	-45.63(15)
Cu01	N005	C00B	C00D	1.95(19)
Cu01	N005	C00B	C00G	-178.27(14)
Cu01	N005	C00I	C00P	178.98(15)
Cu01	N006	C008	C009	3.6(2)
Cu01	N006	C008	C00L	-177.92(15)
Cu01	N006	C00K	C00Q	179.10(16)
N005	C00B	C00D	N004	30.3(2)
N005	C00B	C00G	C00M	-1.1(3)
N005	C00I	C00P	C00M	-0.4(3)
N006	C008	C009	N004	-27.5(2)
N006	C008	C00L	C00O	-1.2(3)
N006	C00K	C00Q	C00O	-1.4(3)
C008	N006	C00K	C00Q	0.1(3)
C008	C00L	C00O	C00Q	-0.1(3)
C009	N004	C00C	C00A	68.34(19)
C009	N004	C00D	C00B	-160.69(15)
C009	C008	C00L	C00O	177.17(19)
C00B	N005	C00I	C00P	-0.4(3)
C00B	C00G	C00M	C00P	0.2(3)
C00C	N004	C009	C008	-88.53(18)
C00C	N004	C00D	C00B	76.20(17)

Atom	Atom	Atom	Atom	Angle/°
C00C	C00A	C00H	C00E	178.65(16)
C00C	C00A	C00N	C00J	-179.24(17)
C00D	N004	C009	C008	149.63(15)
C00D	N004	C00C	C00A	-167.19(15)
C00D	C00B	C00G	C00M	178.64(19)
C00E	C00F	C00J	C00N	-1.0(3)
C00E	C00F	N1	N1[1]	12.5(3)
C00F	C00E	C00H	C00A	0.1(3)
C00F	C00J	C00N	C00A	1.1(3)
C00G	C00B	C00D	N004	-149.49(17)
C00G	C00M	C00P	C00I	0.5(3)
C00H	C00A	C00C	N004	80.1(2)
C00H	C00A	C00N	C00J	-0.6(3)
C00H	C00E	C00F	C00J	0.4(3)
C00H	C00E	C00F	N1	-178.65(17)
C00I	N005	C00B	C00D	-178.55(16)
C00I	N005	C00B	C00G	1.2(3)
C00J	C00F	N1	N1[1]	-166.6(2)
C00K	N006	C008	C009	-177.24(17)
C00K	N006	C008	C00L	1.2(3)
C00L	C008	C009	N004	154.06(18)
C00L	C00O	C00Q	C00K	1.3(3)
C00N	C00A	C00C	N004	-101.2(2)
C00N	C00A	C00H	C00E	0.0(3)
N1	C00F	C00J	C00N	178.12(17)

[1]2-x,1-y,1-z

Table S- 9. Hydrogen Fractional Atomic Coordinates (×10^4) and Equivalent Isotropic Displacement Parameters (Å^2×10^3) for ***E*-1a**. U_{eq} is defined as 1/3 of the trace of the orthogonalised U_{ij}.

Atom	x	y	z	U_{eq}
H00C	3888.74	6272.41	5751.07	33
H00D	3792.02	4916	5697.98	33
H00E	2300.26	5731.32	6451.95	32
H00F	2984.04	5397.76	7146.25	32
H00G	8282.41	3716.38	5425.22	35
H00I	6079.06	3801.96	5758.76	34
H00P	9797.48	7728.94	7285.32	49
H00R	10639.74	5861.93	7458	47
H00A	4920(20)	7179(18)	6649(9)	19(5)
H00O	6030(20)	7300(20)	5545(10)	27(5)
H00K	8180(20)	7110(20)	5227(10)	26(5)
H00B	4760(30)	6620(20)	7274(13)	43(7)
H00M	7320(30)	7910(20)	7027(11)	33(6)
H00J	4500(30)	1730(20)	6595(11)	31(6)
H00Q	2260(30)	970(20)	6245(12)	41(7)
H00L	8950(30)	4330(20)	7319(12)	42(7)
H00N	250(30)	2230(30)	6113(13)	56(8)
H00H	630(30)	4110(20)	6333(12)	36(6)

Table S- 10. Solvent masking (PLATON/SQUEEZE) information for ***E*-1a**.

No	x	y	z	V	e	Content
1	-0.976	0.000	0.500	395.2	87.7	2et2o
2	-0.923	0.500	0.000	395.2	87.7	2et2o

F. NMR spectra

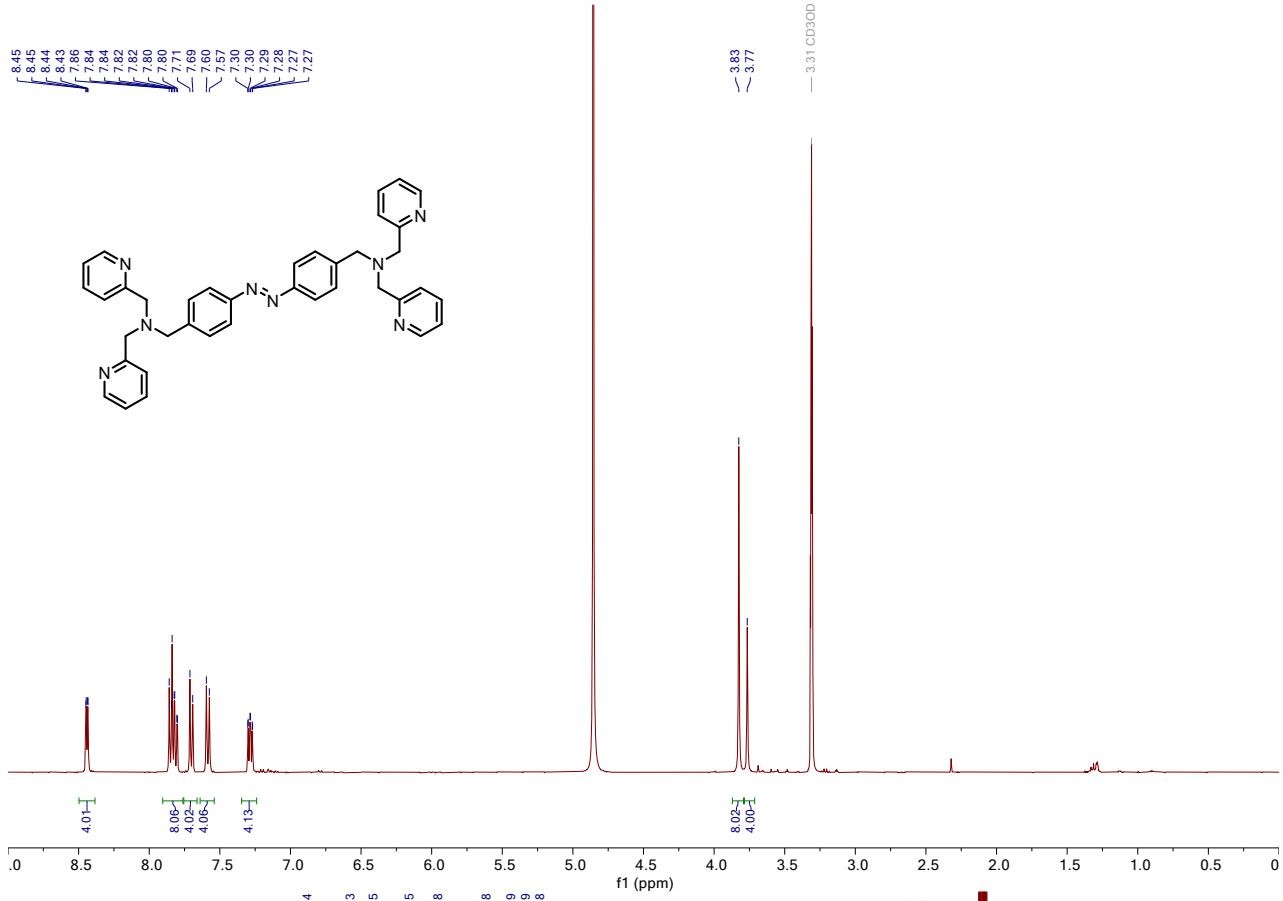

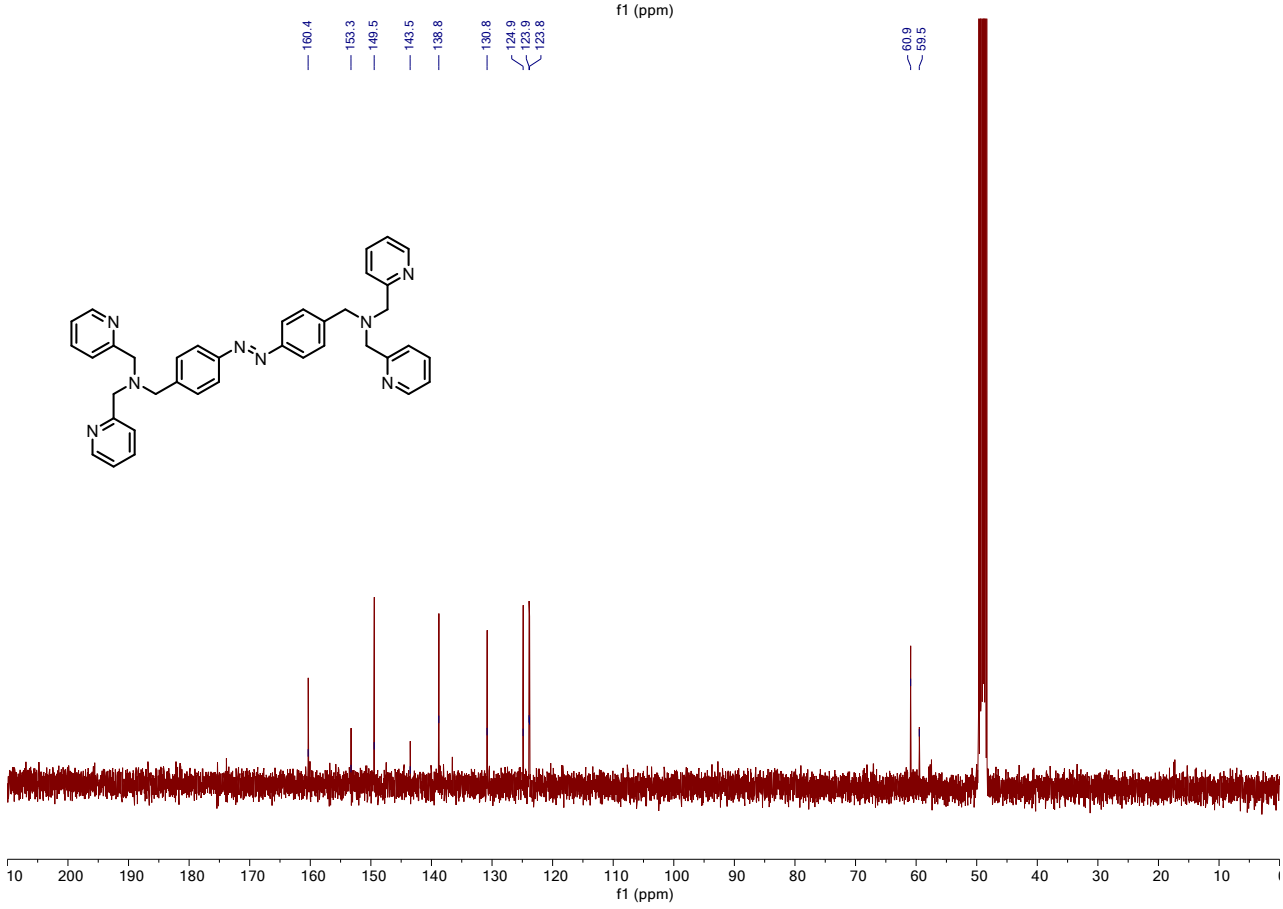

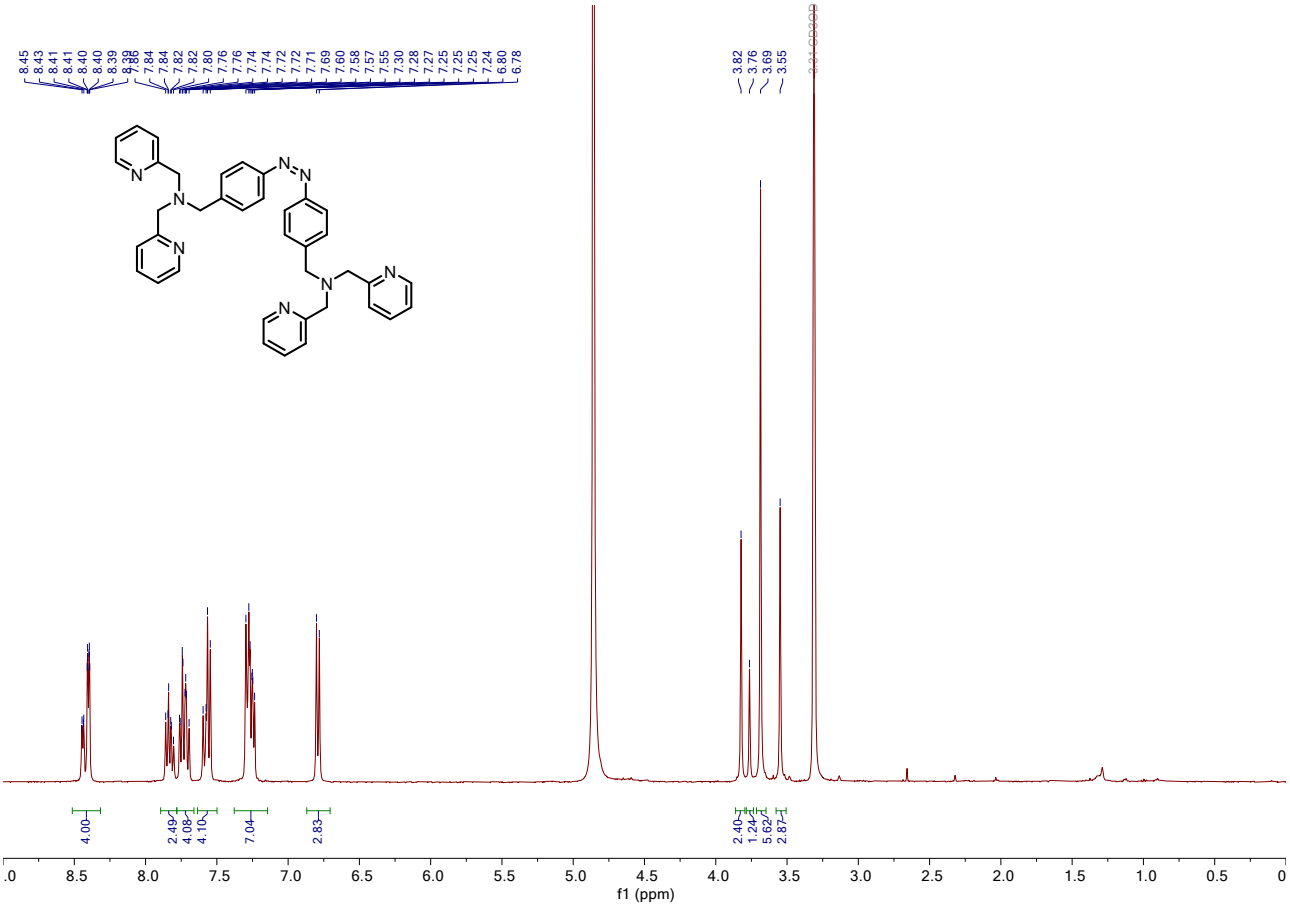
8.45
8.43
8.41
8.41
8.40
8.40
8.39
7.84
7.84
7.82
7.82
7.80
7.76
7.76
7.74
7.74
7.72
7.72
7.71
7.69
7.60
7.58
7.57
7.55
7.30
7.28
7.27
7.25
7.25
7.25
7.24
6.80
6.78
3.82
3.76
3.69
3.55
4.00
2.49
4.08
4.10
7.04
2.83
2.40
1.24
5.62
2.87
f1 (ppm)

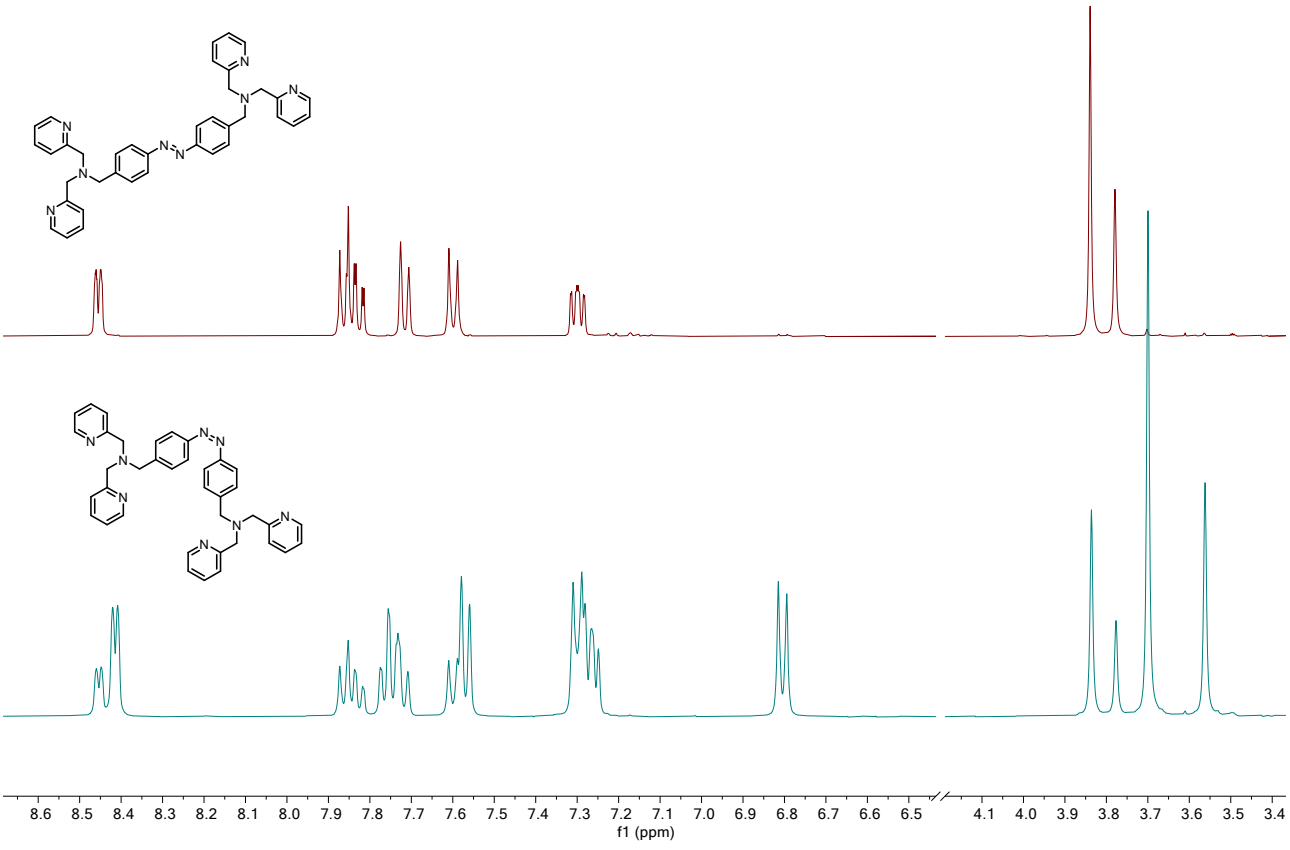
f1 (ppm)

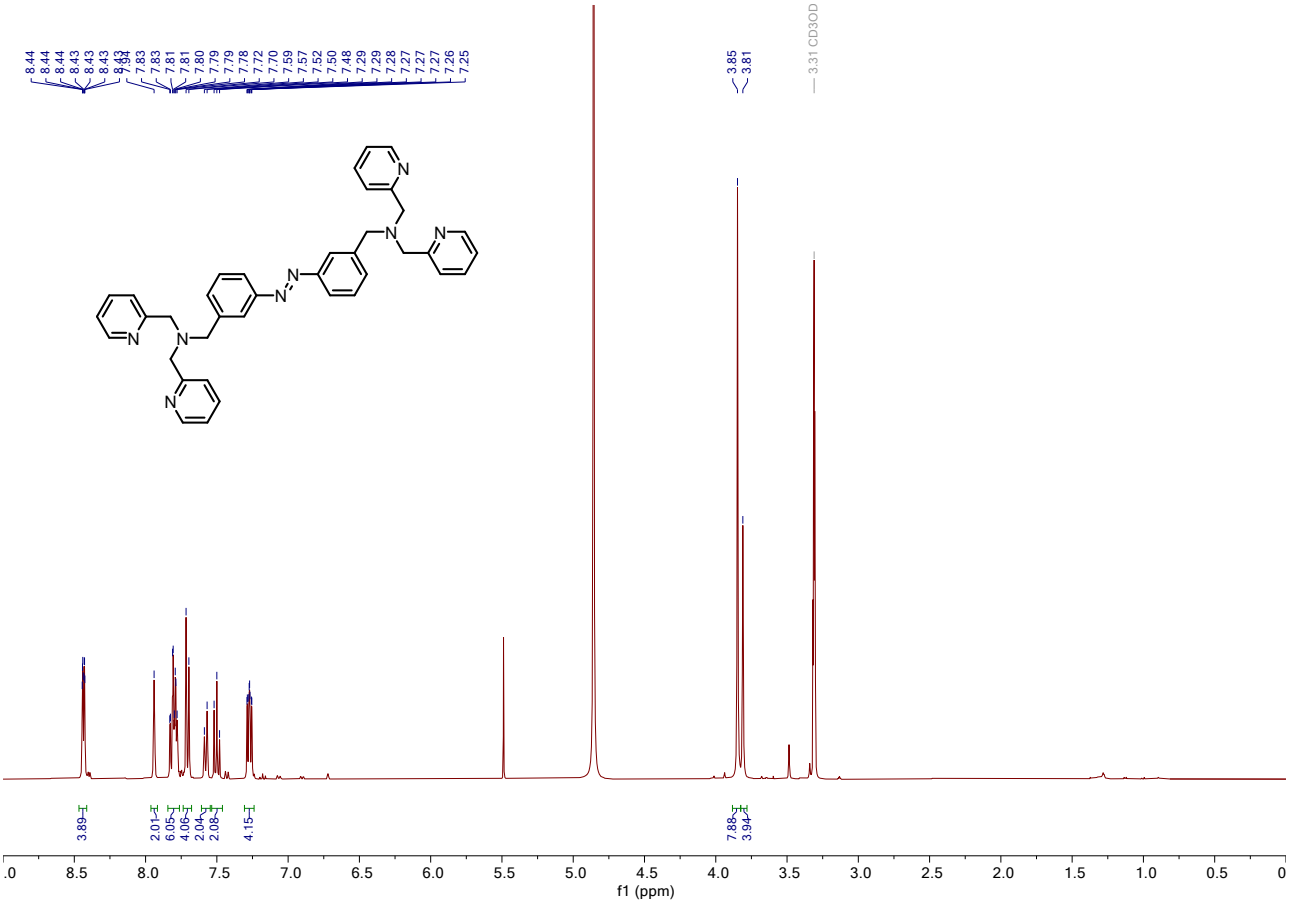
8.44
8.44
8.44
8.43
8.43
8.43
7.83
7.83
7.81
7.81
7.80
7.79
7.79
7.78
7.72
7.70
7.59
7.57
7.52
7.50
7.48
7.29
7.29
7.28
7.27
7.27
7.27
7.26
7.25
3.85
3.81
3.31 CD3OD
3.89
2.01
6.05
4.06
2.04
2.08
4.15
7.88
3.94
f1 (ppm)

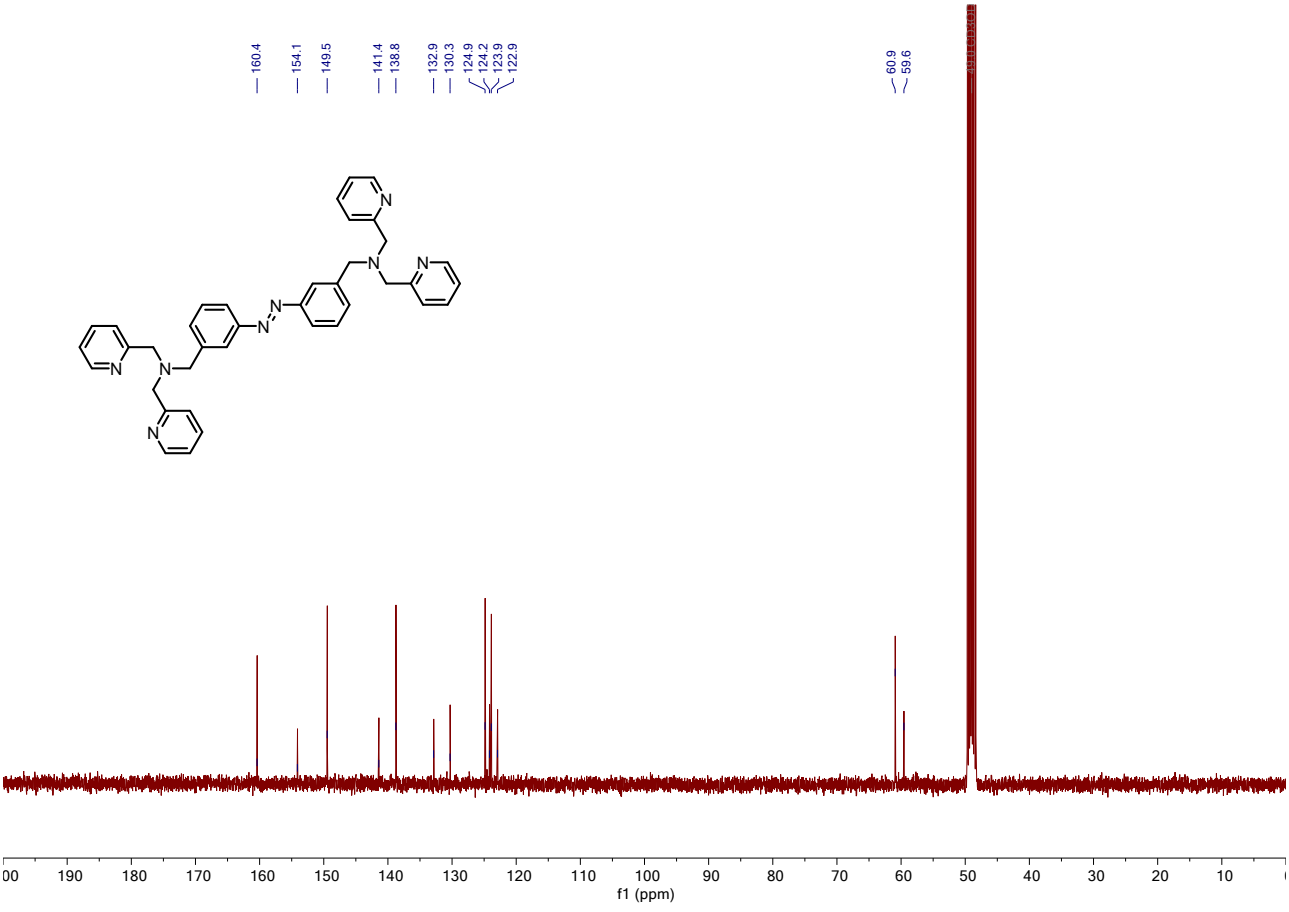
160.4
154.1
149.5
141.4
138.8
132.9
130.3
124.9
124.2
123.9
122.9
60.9
59.6
f1 (ppm)

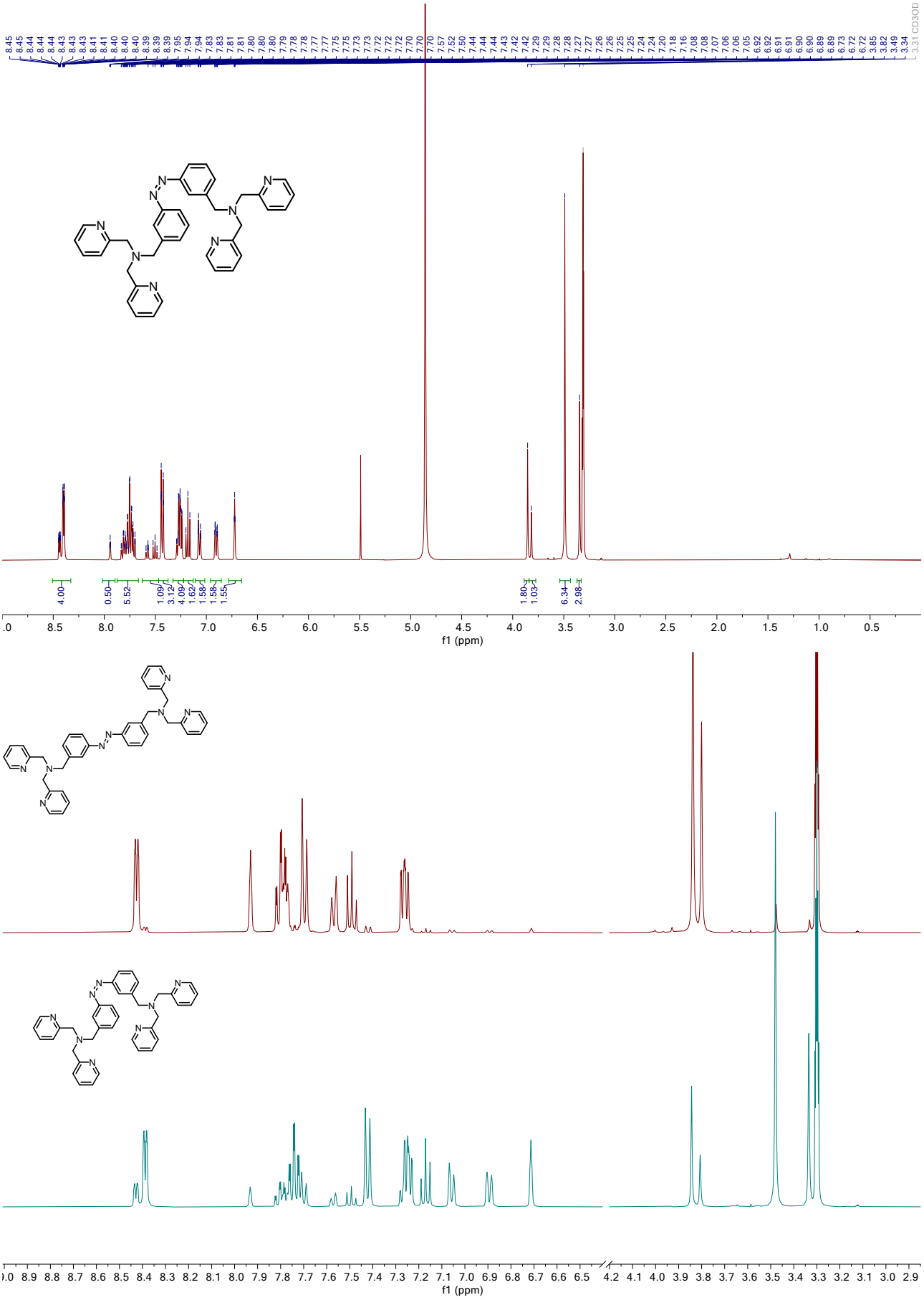
f1 (ppm)
f1 (ppm)

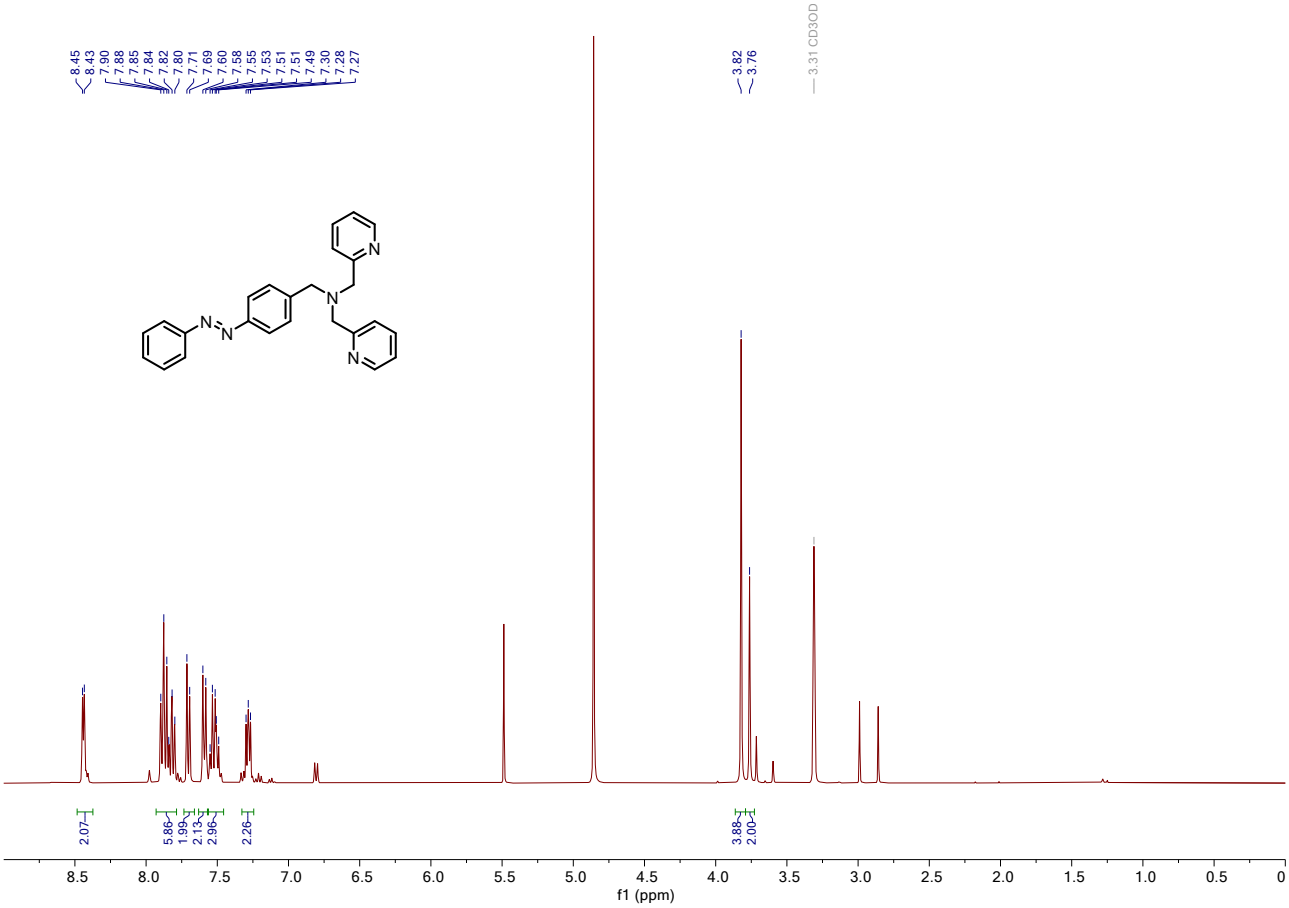
8.45
8.43
7.90
7.88
7.85
7.84
7.82
7.80
7.71
7.69
7.60
7.58
7.55
7.53
7.51
7.51
7.49
7.30
7.28
7.27
3.82
3.76
3.31 CD3OD
2.07
5.86
1.99
2.13
2.96
2.26
3.88
2.00
f1 (ppm)

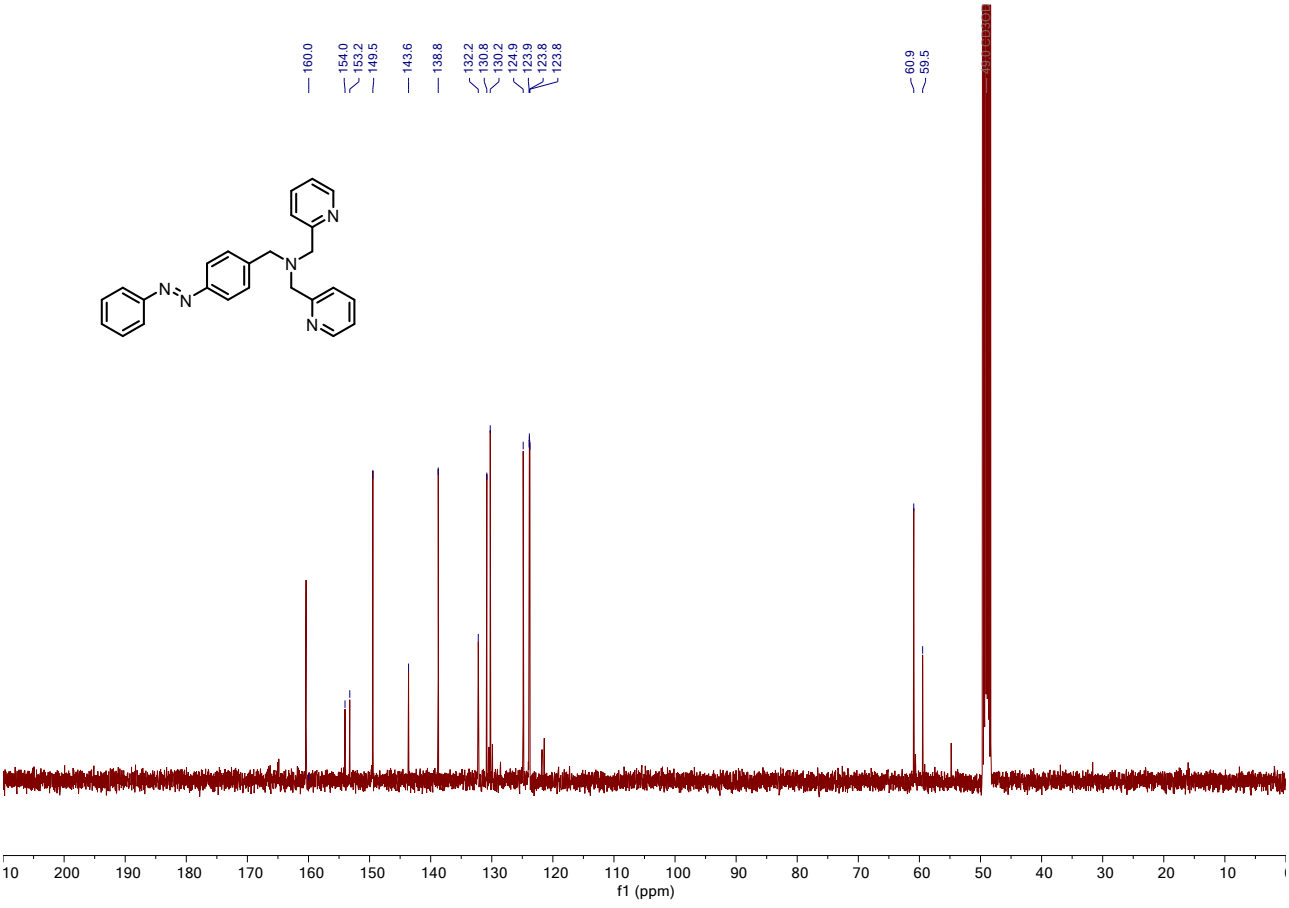
160.0
154.0
153.2
149.5
143.6
138.8
132.2
130.8
130.2
124.9
123.9
123.8
123.8
60.9
59.5
f1 (ppm)

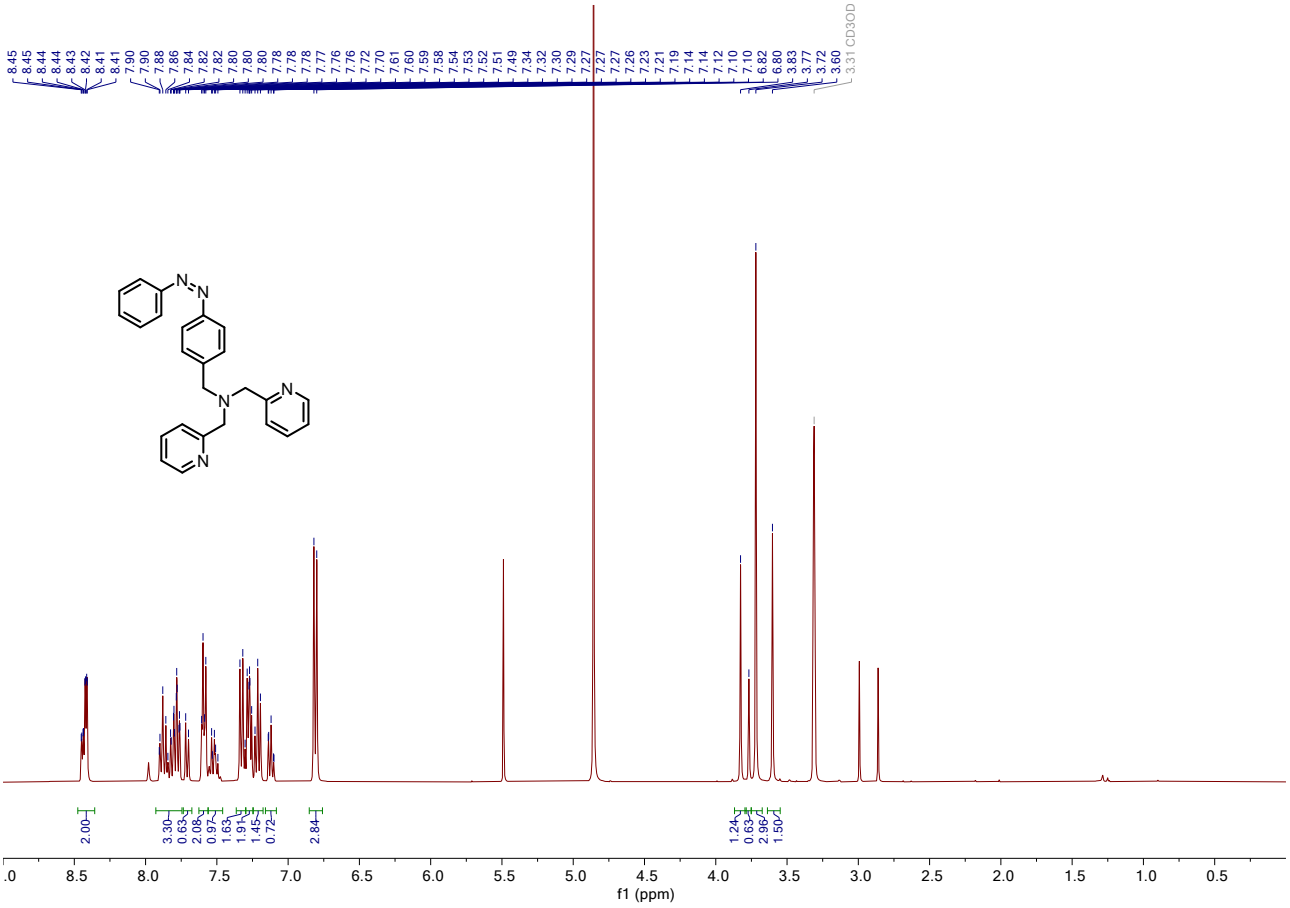
8.45
8.45
8.44
8.44
8.43
8.42
8.41
8.41
7.90
7.90
7.88
7.86
7.84
7.82
7.82
7.80
7.80
7.80
7.78
7.78
7.78
7.77
7.76
7.76
7.72
7.70
7.61
7.60
7.59
7.58
7.54
7.53
7.52
7.51
7.49
7.34
7.32
7.30
7.29
7.27
7.27
7.27
7.26
7.23
7.21
7.19
7.14
7.14
7.12
7.10
7.10
6.82
6.80
3.83
3.77
3.72
3.60
3.31 CD3OD
2.00
3.30
0.63
2.08
0.97
1.63
1.91
1.45
0.72
2.84
1.24
0.63
2.96
1.50
f1 (ppm)

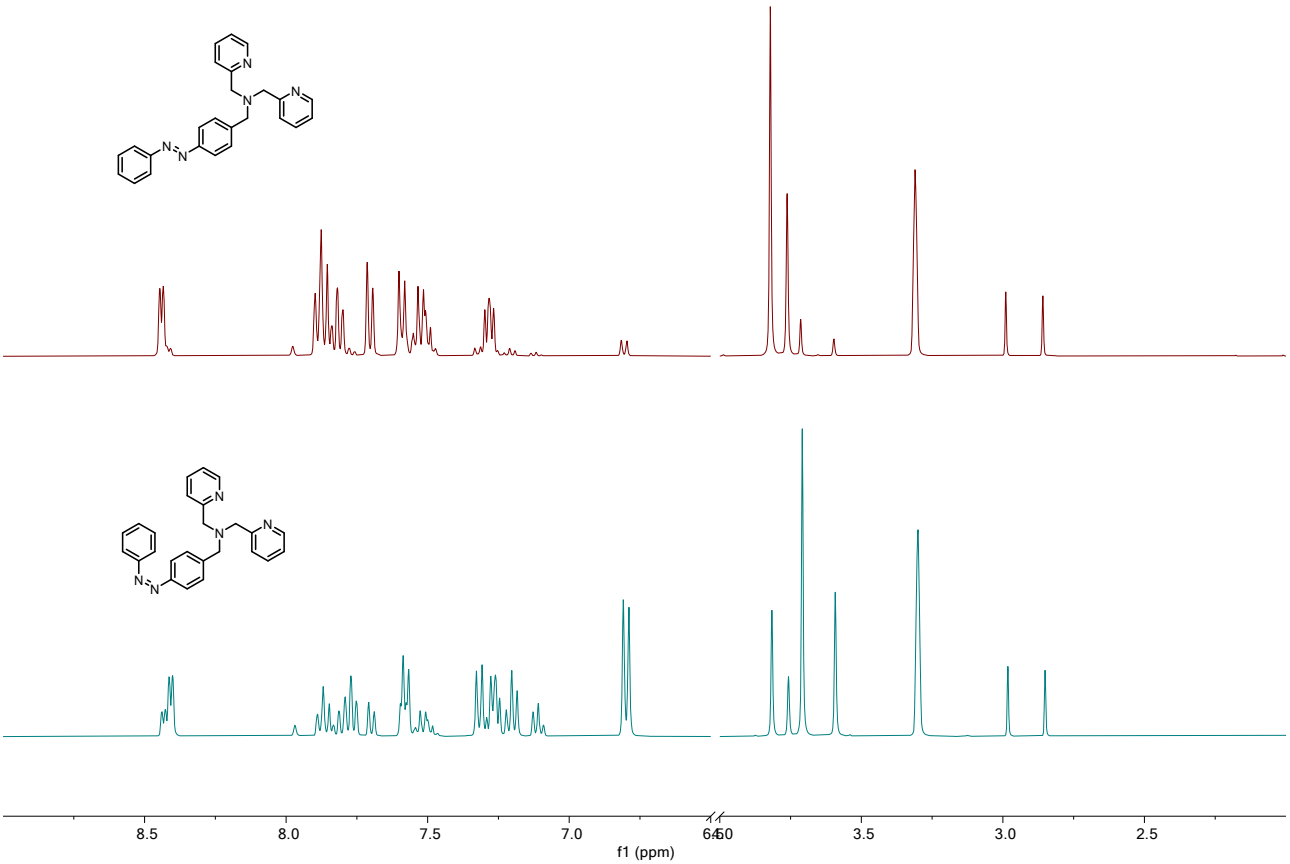
f1 (ppm)

G. IR spectra

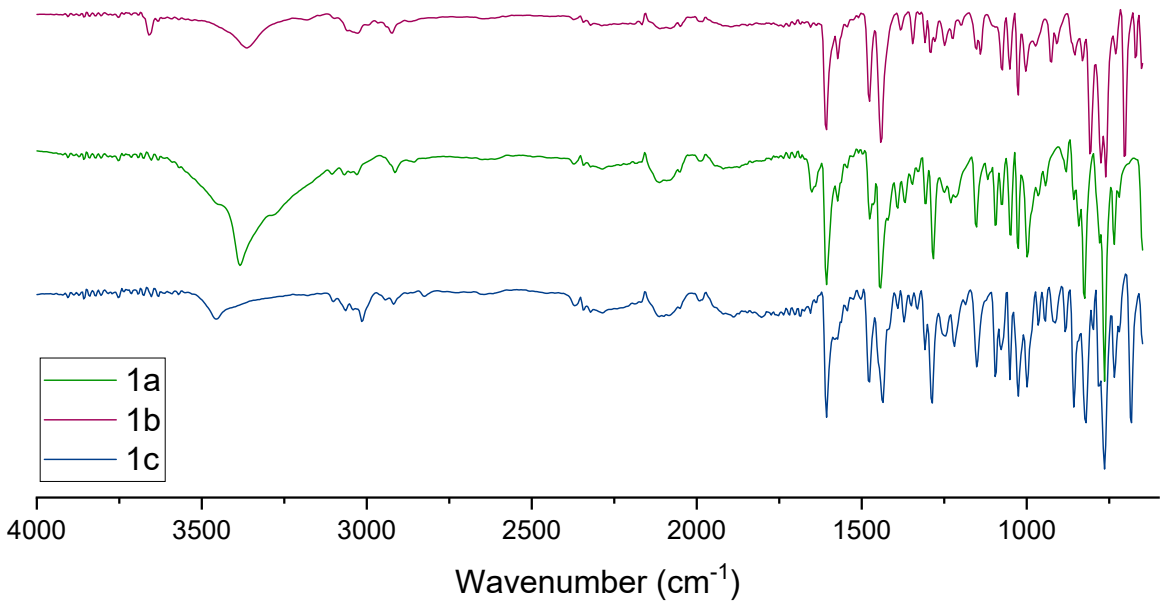

Figure S- 19. FT-IR spectra of **1a**, **1b** and **1c**.

H. Cartesian coordinates

All the cartesian coordinates can be downladed free of charge from Figshare. The associated DOI for the dataset is the following: 10.6084/m9.figshare.21757619.

I. References

1 S. Grimme, A. Hansen, S. Ehlert and J.-M. Mewes, *J. Chem. Phys.*, 2021, **154**, 064103.

2 F. Neese, F. Wennmohs, U. Becker and C. Riplinger, *J. Chem. Phys.*, 2020, **152**, 224108.

3 B. Priewisch and K. Rück-Braun, *J. Org. Chem.*, 2005, **70**, 2350–2352.

4 F. Riefolo, C. Matera, A. Garrido-Charles, A. M. J. Gomila, R. Sortino, L. Agnetta, E. Claro, R. Masgrau, U. Holzgrabe, M. Batlle, M. Decker, E. Guasch and P. Gorostiza, *J. Am. Chem. Soc.*, 2019, **141**, 7628–7636.

5 N. A. Simeth, T. Kinateder, C. Rajendran, J. Nazet, R. Merkl, R. Sterner, B. König and A. C. Kneuttinger, *Chem. – A Eur. J.*, 2021, **27**, 2439–2451.

6 G. Sheldrick, *Acta Crystallogr. Sect. A*, 2015, **71**, 3–8.

7 O. V Dolomanov, L. J. Bourhis, R. J. Gildea, J. A. K. Howard and H. Puschmann, *J. Appl. Crystallogr.*, 2009, **42**, 339–341.

8 G. Sheldrick, *Acta Crystallogr. Sect. C*, 2015, **71**, 3–8.